Ore Geology Reviews 58 (2014) 126–147

Contents lists available at ScienceDirect

Ore Geology Reviews

journal homepage: www.elsevier.com/locate/oregeorev

Review

# Characterization of apatite resources in Norway and their REE potential — A review

Peter M. Ihlen *, Henrik Schiellerup, Håvard Gautneb, Øyvind Skår

*Geological Survey of Norway, P.O. Box 6315 Sluppen, NO-7491 Trondheim, Norway*

ARTICLE INFO

*Article history:*
Received 23 May 2013
Received in revised form 7 November 2013
Accepted 10 November 2013
Available online 16 November 2013

*Keywords:*
Igneous apatite deposits
Sedimentary phosphates
Apatite veins
REE–Y–Th
Norway

ABSTRACT

Apatite is a necessity for the production of phosphorus fertilizers and presents a potential raw material for the extraction of REE and Y. A wide spectrum of apatite deposits is found in Norway including sedimentary, igneous, and vein type deposits. The igneous deposits which appear to have the greatest potential for exploitation occur associated with alkaline complexes, massif-type anorthosite complexes and monzonitic complexes. One of the most promising is found in the monzonoritic Bjerkreim–Sokndal Layered Intrusion of the early Neoproterozoic Rogaland Anorthosite Province in southwest Norway. The intrusion hosts three cumulate units with high-grade ore zones. The most promising resource is confined to MCU IV which is 50–170 m thick and nearly 10 km long with average normative contents of 10.2% apatite, 12.4% ilmenite and 7.3% vanadium-rich magnetite. The late Neoproterozoic–Cambrian carbonatite-bearing alkaline complexes are generally of low grade to represent potential resources of apatite as the sole commodity. However, apatite may represent a byproduct of potential Nb and REE + Y mineralisation in the Fen Complex in southern Norway. The late Ordovician–Silurian Misværdal complex comprising multiple alkali clinopyroxenite intrusions in the Uppermost Allochthon of the Caledonides in northern Norway contains 1–1.5 km long and 100–200 m wide ultrapotassic clinopyroxenite dykes with average contents of 7–10 wt.% apatite and with intermediate levels of TREY (~0.5 wt.%). However, high levels of Th in the apatite make it less suitable as a raw material for fertilizer production. Apatite–Fe–Ti oxide ores being characteristic for the monzonitic complexes are especially well developed in the Permian Oslo Igneous Province where apatite-rich magnetite clinopyroxenite cumulates are found in the Larvik Plutonic Complex. The Kodal body has an inferred open-pit ore reserve calculated to 70 Mt with approximately 11.6 wt.% apatite, 3.0 wt.% ilmenite and 26.5 wt.% ilmenomagnetite. The apatite contains about 1 wt.% REE. Comparable types of deposits of Palaeoproterozoic age have recently been recognized in the alkali-calcic mangeritic to syenitic intrusions in the Lofoten–Vesterålen Mangerite Complex in northern Norway, whereas complexes with variable proportions of anorthosites (s.s.), jotunites and mangerites occurring in the Middle Allochthon of the Caledonides in South Norway also are known to host apatite-bearing Fe–Ti oxide deposits, some high in apatite. These complexes represent potential areas for green-field exploration. The TREY (TREE + Y) contents of the apatite in the igneous deposits are discussed and comprise very low levels in the Bjerkreim–Sokndal Layered Intrusion, intermediate levels in the carbonatites and pyroxenites of the alkaline complexes as well as nelsonite dykes and mangerite-associated deposits to high levels in the monzonite-associated deposits.

© 2013 Elsevier B.V. All rights reserved.

**Contents**

1. Introduction . . . 127
2. Geological setting . . . 127
3. Sedimentary deposits . . . 129
   3.1. Stratiform Fe-oxide–apatite deposits . . . 129
   3.2. Phosphorite occurrences . . . 130
4. Igneous deposits . . . 130
   4.1. Deposits in alkaline complexes . . . 130
      4.1.1. The Fen Complex . . . 130
      4.1.2. Alkaline complexes of the Seiland Igneous Province . . . 132
      4.1.3. The Misværdal Complex . . . 135

* Corresponding author. Tel.: +47 92255809.
*E-mail address:* peter.ihlen@ngu.no (P.M. Ihlen).

0169-1368/$ – see front matter © 2013 Elsevier B.V. All rights reserved.
http://dx.doi.org/10.1016/j.oregeorev.2013.11.003

4.2. Deposits in massif-type anorthosite complexes . . . 137
4.2.1. The Rogaland Anorthosite Province . . . 137
4.3. Deposits in monzonitic complexes . . . 140
4.3.1. Apatite–Fe–Ti ores in the Lofoten–Vesterålen Mangerite Complex . . . 141
4.3.2. Apatite–Fe–Ti ores in the Larvik Plutonic Complex . . . 141
5. Vein deposits . . . 142
5.1. Kiruna-type apatite–Fe oxide deposits . . . 142
5.2. Metasomatic deposits . . . 142
6. The REE chemistry of apatite . . . 143
7. Conclusion . . . 144
Acknowledgment . . . 145
References . . . 145

## 1. Introduction

Apatite [$Ca_5(PO_4, CO_3)_3(OH, F, Cl)$] is the most abundant crystalline phosphate mineral which is found as an accessory mineral in most rock types on the earth surface. However, exploitable deposits of apatite are mainly found in sedimentary and igneous rocks. The former comprises stratiform phosphorite deposits in shelf-type shale-carbonate sequences that contain high-phosphorous ores of microcrystalline $CO_2$-rich fluorapatite (francolite) and cryptocrystalline collophane. The igneous deposits comprise fluorapatite ores which are mostly hosted by carbonatites and other types of alkaline intrusions. The magmatic ores are generally of lower grade, but give higher quality beneficiation products with low contents of unwanted contaminants (Cd, As, U, Th, Mg, and Al).

Beneficiation products of apatite ores as a commodity are traded as phosphate rock. It is the only significant global resource of phosphorus used dominantly in the manufacturing of nitrogen–phosphorus–potassium (NPK) fertilizers for food-crop nutrition and the production of animal feed supplements. Only 10–15% of the world production of phosphate rock has other applications (e.g. pharmaceuticals, ceramics, textiles and explosives). Sedimentary apatite rock makes the largest contribution to the world production of about 210 Mt (2012) whereas igneous apatite rock accounts for only 10–15% of this total (Jasinski, 2011, 2013). Although present resources of phosphate rock are large, the general high demand has over the years lead to a progressive depletion of high-grade ores and ores of good quality with few contaminants. In general, the phosphate content of economic ore appears to have decreased by about 0.45 wt.% $P_2O_5$ per decade. The economic grade of a sizeable igneous apatite deposit is now 4–5 wt.% $P_2O_5$.

Presently, there is no production of phosphate rock in Norway and has in the past been of minor importance. Today, Yara International ASA which operates two NPK-fertilizer plants in Norway imports large volumes of phosphate rock. In spite of a long standing production of NPK-fertilizers by the company and its forerunner Norsk Hydro few efforts have been made to explore potential apatite provinces in Norway. However, renewed interest for potential apatite resources in Norway occurred when China, the dominant producer of REE in the world, implemented export restrictions for REE products in 2008. In the rest of the world, this lead to intensified search for alternative sources of REE, including deposits of LREE-enriched apatite [$(Ca, LREE)_5(PO_4, SiO_4)_3(F)$] normally found in igneous deposits. Magmatic apatite contains commonly more than 0.35 wt.% REE or 0.4 wt.% REO (see Tables 3 and 4). According to the mineral production statistics given by Brown et al. (2013) and Jasinski (2013) the world production of apatite from igneous deposits in 2011 was 20–30 Mt. If 25 Mt is estimated to contain apatite with an average content of 0.5 wt.% REO, the total amount of REO residing in the world production of igneous apatite would be approximately125,000 tonnes with predominance of LREO. This is roughly equal to the world production of REO in 2011 which suggests that extraction of REE from apatite as a byproduct of NPK-fertilizer production represents an important alternative source of REE.

In Norway a number of geological provinces with a wide variety of apatite deposits are currently investigated by Norges geologiske undersøkelse (NGU; Geological Survey of Norway) including the REE contents of apatite. The present paper is based on unpublished results of on-going NGU projects and from data given in published papers, NGU reports, Norsk Hydro internal prospecting reports archived at NGU, NGU Ore Database and NGU Industrial Mineral Database. Most of these data are stored in NGU archives and reports are given in Norwegian like most of previously published accounts on the occurrence of apatite in Norway, e.g., Neumann (1985). Thus, the aim of the present paper is to present for the first time an up to date overview in English of phosphate deposits in Norway and their resources.

## 2. Geological setting

Norway is situated on the western margin of the Fennoscandian Shield which comprises an Archaean cratonic nucleus with Palaeoproterozoic greenstone belts in the northwest being fringed by successively younger mobile belts towards the southwest (Fig. 1). These include the Palaeoproterozoic Svecofennian mobile belt in the central part and the Late Mesoproterozoic–Early Neoproterozoic Sveconorwegian mobile belt (SMB) in the southwest. These two mobile belts are separated by the Transscandinavian Igneous Belt (TIB) which developed episodically over the period 1860–1650 Ma in a convergent continental-margin setting (Andersson et al., 2004, and references therein). The Archaean and Proterozoic mega-units are to a large part covered by nappe complexes of the Norwegian Caledonides and younger rocks of the Late Carboniferous–Early Triassic Oslo Paleorift including the Oslo Igneous Province (OIP) along the centre of the rift grabens.

The Fennoscandian Shield contains a large diversity of ore deposits and represents a major producer of metals and industrial-mineral raw materials in Europe. In 2013, the three sole producers in Europe of high-grade igneous phosphate rock are found at Siillinjärvi in Finland (Fig. 1) and at Kirovsk and Kovdor in Russia where an Archean carbonatite and Devonian alkaline complexes with nepheline syenite and phoscorite are being worked, repectively (Ilyin, 1989; Puustinen and Kauppinen, 1989). The apatite deposits in the Norwegian part of the Shield comprise sedimentary, igneous and vein type deposits (Table 1). The first two are largely syngenetic whereas the latter is epigenetic. Potential apatite resources are only found associated with the igneous deposits which occur mainly in the SMB, in the plutonic rocks of the OIP, in the TIB intrusions, and in the Caledonides in order of potential economic importance.

The TIB comprises dominantly batholithic massifs of monzonitic to granitic composition intruding comagmatic volcanites. The majority of the plutonic rocks in the belt have sub-alkaline and alkali-calcic chemistry with I-type signature that in some areas may comprise A-type and rarely S-type varieties (Andersson et al., 2004). The batholiths of alkali-calcic mangerites (opx. monzonites) and monzonites (Malm and Ormaasen, 1978) of the Lofoten–Vesterålen Mangerite Complex (Fig. 1, LVMC) in the northern extension of the TIB contain abundant

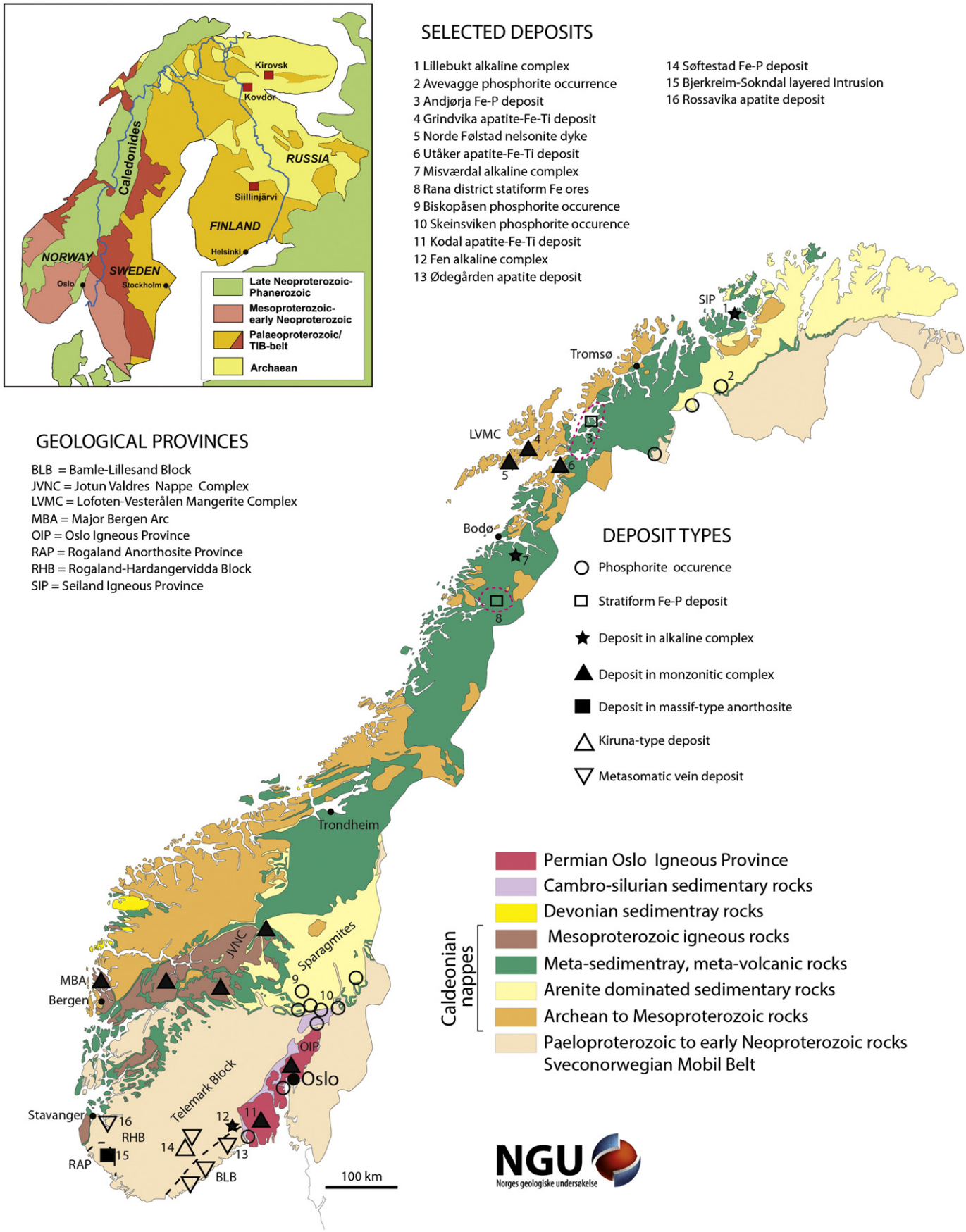


**Fig. 1.** Simplified geological map of Norway showing the distribution of apatite deposits and important provinces with abbreviations used in the text where the numbered deposits are mentioned. Key map depicts the main mega-tectonic units of the Fennoscandian shield and the continent Baltica.

**Table 1**
Summary data of deposits and areas mentioned in the text together with an assessment of their economic potential. Abbreviations: BLB = Bamble–Lillesand Block, JVNC = Jotun–Valdres Nappe Complex, LA = Lower Allochthon, LVMC = Lofoten–Vesterålen Mangerite Complex, MA = Middle Allochthon, MBA = Major Bergen Arc, RHB = Rogaland–Hardangervidda Block, POT. = potential, SMB = Sveconorwegian Mobile Belt, TB = Telemark Block, TIB = Transscandinavian Igneous Belt, UmA = Uppermost Allochthon.

| Type of deposit | Subtype | Province | Deposit/Occurrence | Main commodity | Potential byproduct | Econ pot |
|---|---|---|---|---|---|---|
| Sedimentary | Phosphorite | LA, Caledonides/Caledonian front | Biskopasen | Phosphate | | No |
| | | | Avevagge | Phosphate | | No |
| | | | Steinsviken | Phosphate | | No |
| | Stratiform Fe–P | UmA, Caledonides | Andørja | Magnetite | Apatite | Low |
| Igneous | Carbonatite | TB, SMB | Fen | Nb, REE | Apatite | Mod. |
| | | MA, Caledonides | Lillebukt | Apatite | | Low |
| | Alkali pyroxenite | MA, Caledonides | Lillebukt | Apatite | | Low |
| | Pegmatitic gabbro | MA, Caledonides | Tappeluft | Apatite | | Low |
| | High-K pyroxenite | UmA, Caledonides | Misværdal | Apatite | REE | L.-Mod. |
| | Monzonite | Oslo Igneous Province | Kodal | Apatite | REE, (Fe, Ti) | High |
| | Mangerite | LVMC, TIB | Grindvika | Apatite, | REE, (Fe, Ti), | Not determined |
| | | MA, Caledonides | JVNC | Apatite, | REE? (Fe, Ti), | |
| | | MA, Caledonides | MBA | Apatite | REE? (Fe, Ti) | |
| | Layered leuconorite | Rogaland Anorthosite Province | Bjerkreim–Sokndal | Apatite, ilmenite | V-magnetite | High |
| Vein | Kiruna-type Fe–P | TB, SMB | Søftestad | Magnetite | Apatite | Low |
| | Metasomatic | BLB, SMB | Ødegarden | Apatite | REE | No |
| | | RHB, SMB | Rossavika | Apatite | | No |

occurrences of Fe–Ti–P (nos. 4–6, Fig. 1). It was regarded by Gorbatschev (2004) to be part of the TIB plutons, though noting their association with abundant gabbroic and anorthositic intrusions and the absence of coeval volcanites uncommon in other parts of the belt. The rocks within the SMB were formed during the Mesoproterozoic (~1600–1050 Ma) as a consequence of southwestward accretion of arc sequences truncated by calc-alkaline granitoid intrusions (Andersen et al., 2004; Slagstad et al., 2013). Locally these volcanosedimentary sequences contain Kiruna-type magnetite–apatite ores (no. 14). The present distribution of medium- to high-grade gneiss complexes in the SMB is the ultimate result of the Sveconorwegian orogeny (1140–900 Ma) when the crust became reworked and separated into a number of blocks, sectors, segments or terranes bordered by major shear zones (Andersen, 2005; Bingen et al., 2008; Slagstad et al., 2013). Some of these shear belts are characterized by wide-spread metasomatic rocks and vein deposits of apatite as in the Bamble–Lillesand Block (BLB) where the Ødegården vein deposit is situated (no. 13). The Sveconorwegian orogeny was terminated with the emplacement of post-orogenic granite massifs and anorthosite massifs in the Rogaland Anorthosite Province (RAP; Marker et al., 2003) where apatite-rich jotunitic rocks (opx. monzodiorites) occur, including the Bjerkreim–Sokndal Layered Intrusion (no. 15).

The Caledonian nappes overlay a thin veneer of autochthonous and parautochthonous sedimentary cover sequences of late Neoproterozoic and Cambrian age that contain thin beds of phosphorites along the Caledonian front (e.g. in the Lake Mjøsa district, nos. 9 and10). The final amalgamation of the nappes occurred during the Scandian orogenic event in the Silurian when continent–continent collision occurred between Laurentia and Baltica. The nappes are subdivided into four allochthonous mega-units. The two upper allochthons are composed of terranes exotic to Baltica, whereas the two lower allochthons comprise terranes of Baltic affinity (Roberts, 1988). The Lower Allochthon with scattered phosphorite beds represents a stack of both short- and long-transported units of the underlying autochthonous sedimentary sequences. The Middle Allochthon with abundant arenaceous units is characterized by the presence of tectonic slices of the Proterozoic basement containing Fe–Ti–P deposits in conjunction with jotunite–mangerite intrusions now residing in the Major Bergen Arc (MBA) and the Jotun–Valdres Nappe Complex (JVNC) in southern Norway (Fig. 1). This allochthon comprises, in northernmost Norway, the Seiland Igneous Province (SIP) containing Ediacaran intrusions of apatite-enriched carbonatites and alkalipyroxenites (e.g. Lillebukt, no. 1, Fig. 1). These intrusions are somewhat younger than the apatite-rich Fen Complex in the SMB of southern Norway (no. 12), but both probably formed in response to the break-up of the supercontinent Rhodinia in the Ediacaran–Cambrian time. The Upper Allochthon is composed of abundant Early Palaeozoic volcanic belts which appear devoid of apatite except in northern Norway where it contains Neoproterozoic meta-sedimentary sequences with stratiform Fe, Fe–Mn and Fe–P ores comparable to those in the Uppermost Allochthon (no. 3). In northern Norway the latter is dominated by Late Neoproterozoic (700–600 Ma) carbonate-mica schist sequences truncated by Ordovician–Silurian granitic batholiths and locally associated apatite-rich ultrapotassic pyroxenite intrusions (Misværdal, no. 7).

The Carboniferous to Triassic OIP comprises saturated to undersaturated alkaline to subalkaline basaltic, latitic, trachytic and ignimbritic volcanites formed in conjunction with fissure eruptions and subsequent formation of central volcanoes with associated calderas. The volcanites are truncated by gabbroic, monzonitic, syenitic and granitic plutons. The early Permian monzonite plutons and associated monzodiorites contain especially in the southern part of the palaeorift abundant accumulations of apatite–Fe–Ti ores which include the Kodal deposit (no. 11).

The present landscape in Norway and Fennoscandia is strongly influenced by numerous episodes of glaciation in the Pleistocene and Holocene when a surface of Mesozoic–Tertiary deep weathering was eroded, leaving widely distributed remnants of weathered rocks including some hosting phosphate deposits dealt with below.

## 3. Sedimentary deposits

### 3.1. Stratiform Fe-oxide–apatite deposits

The deposits are part of a group of iron formations developed worldwide during the end of the Neoproterozoic. These deposits are characterized by enrichment of manganese and phosphorus and were deposited in conjunction with periods of mantle plume activity and global glaciations (Bekker et al., 2010). They are common in the Uppermost and partly Upper Allochthons of the Caledonides of northern Norway where they form stratiform units intercalated with different types of amphibolite facies mica schists and calcitic to dolomitic marbles of late Neoproterozoic age (700–590 Ma; Melezhik et al., 2003; Melezhik, pers. com., 2013). Subordinate meta-volcanic rocks are commonly found in close proximity to the ore horizons. They include amphibolites and various types of biotite–hornblende gneisses of basaltic to dacitic compositions and showing chemical signatures transitional between ocean-floor and calc-alkaline basalts, i.e. an immature arc–back arc setting. The isoclinally folded and dismembered ore horizons are frequently developed as Banded Iron Formations (BIF) with alternating bands (mm–dm scale) dominated by magnetite/hematite, quartz, garnet, and/or calcic amphibole, as well as locally grunerite and ankerite (Bugge, 1948; Foslie, 1949). Their association with meta-volcanic

rocks suggests that the iron ores originated as chemical sediments deposited from Fe–Mn-rich hydrothermal plumes generated in conjunction with sub-aqueous volcanism.

The iron ores can be subdivided into two major types on the basis of their average $P_2O_5$ contents including high-P (>0.7 wt.% $P_2O_5$) and low-P (<0.7 wt.% $P_2O_5$) ores. These two types of ore are often found at different levels in the tectonostratigraphy (Bugge, 1978). The low-P ores presently being mined in the Rana district (no. 8 in Fig. 1) are frequently bordered by Mn-silicate-banded (garnet-rich) units. The high-P ores are characterized by low contents of manganese (<0.2 wt.% MnO). The largest of the explored high-P deposits is the Andørja deposit (no. 3 in Fig. 1) in Troms comprising 8 closely spaced and 7.5–30 m thick ore horizons hosted by biotite amphibolites over a distance of about 2 km (Geis, 1967; Lindahl and Priesemann, 1999). Estimated reserves based on 125 drill holes are 91 Mt with 11.1–22.1 $Fe_{mag}$ and 1.9–2.7 wt.% $P_2O_5$. The fluorocarbonate apatite with 0.23 wt.% Cl is unsuitable for fertilizer production (<0.2 wt.% Cl) and contains only 572 ppm total REE (TREE) and 206 ppm Y (Lindahl and Priesemann, 1999) that are comparable with the contents in the apatite of the Rana district (Bugge, 1978).

### 3.2. Phosphorite occurrences

The earliest of several major episodes of phosphogenesis in the earth history, i.e. in the latest Neoproterozoic and Cambrian (Cook and McIlhinney, 1979) has left its finger print in the form of thin beds of phosphatic glauconite sandstones and phosphoritic conglomerates representing littorial to shallow marine deposits. These occur mainly in the Neoproterozoic sedimentary sequences of intercalated shales, feldspatic sandstones and arkoses (sparagmites) in the Lake Mjøsa District and in the Cambro-Ordovician shale-carbonate sequences along the margin of the OIP (Bjørlykke, 1974; Bjørlykke et al., 1976; Neumann, 1985). The thickest of these phosphatic units is part the Neoproterozoic sub-marine fan at Biskopåsen (no. 9 in Fig. 1) where a 10–20 m thick basal sequence of grain-supported conglomerates contains abundant immature angular clasts and poorly rounded pebbles of limestone and phosphorite (1–10 cm in diameter; Bjørlykke et al., 1976, and references therein).

The Cambrian succession carries phosphate-enriched beds in the basal shale–sandstone sequences covering the weathered Proterozoic gneiss complexes along the sub-Cambrian peneplain/unconformity. The sandstone beds rarely exceeding a few metres in thickness contain phosphorite nodules and phosphatic fossil detritus as well as several interlayered conglomeratic beds (cm to dm thick) with clasts of phosphatic sandstones and phosphorites (Neumann, 1985, and references therein). The thickest sequences of Early Cambrian age are found in the autochthonous Dividalen Group in Reisadalen of northern Norway (no. 2) where a 100–150 m thick sequence of sandstones and siltstones comprises phosphate-cemented units with scattered phosphorite ooliths, concretions and thin beds of phosphorite conglomerates (Vogt, 1967; Vrålstad, 1976). Grab sampling of these sandstones by Norsk Hydro at Avevagge gave a maximum of 2.0 wt.% $P_2O_5$ (Vrålstad, 1976).

Comparable low-grade phosphatic units (<1 m thick) are also found along unconformities at the base of the Middle Cambrian, the Middle Ordovician and of the Upper Ordovician (Neumann, 1985). The Middle Cambrian sandstone bed and overlying phosphorite-pebble conglomerate at Steinsviken, Lake Mjøsa, (no. 10) contain 2.1 wt.% and 6.69 wt.% $P_2O_5$, respectively (Strand, 1929, and references therein). Although REE analyses have not yet been conducted, all of the known occurrences have too small dimensions and phosphate grades to be of economic interest.

## 4. Igneous deposits

### 4.1. Deposits in alkaline complexes

The alkaline complexes in Norway range in age from the Palaeoproterozoic to the Silurian and include those at Fen, Seiland Igneous Province (SIP) and Misværdal treated below (nos. 12, 1 and 7, respectively). These complexes show different ratios of carbonatites versus magmatic silicate rocks that are highest in the former complex and lowest in the latter. All the complexes are enriched in apatite, but differ in contents of high field strength elements (e.g. Y, REE, Th, Nb) which occur strongly enriched in the Fen carbonatites, but are comparably low in the Lillebukt (SIP) and Misværdal complexes.

#### 4.1.1. The Fen Complex

The Fen Complex has become famous by the pioneering work by Brøgger (1921) who recognized carbonatites as a specific group of magmatic rocks and established it among the type examples of its kind.

*4.1.1.1. Geological outline.* The Fen Complex is situated in Mesoproterozoic granitic orthogneisses about 17 km west of the southwestern margin of the OIP (Figs. 1 and 2). It is surrounded by a wide halo (1500 $km^2$) of small satellite intrusions and dykes of similar composition as the rocks of the central complex (Bergstøl and Svinndal, 1960; Dahlgren, 1987, 2004). Meert et al. (1998) advocated on the basis of their own $^{40}Ar/^{39}Ar$ dating of phlogopites in ultramafic lamprophyre (damtjernite) and phonolite satellites that the best estimate for the emplacement of the complex is 583 ± 10 Ma or late Neoproterozoic (Ediacaran). The emplacement occurred at shallow level in the crust and probably at a 1–3 km depth below the sub-Cambrian peneplain (Sæther, 1957). Gravity data indicates that the central complex is underlain by a pipe-shaped body of dense material, probably mafic–ultramafic silicate rocks extending from a few hundred metres below the present surface to at least 15 km in depth (Ramberg, 1973).

The central complex comprises an about 9 $km^2$ sub-circular composite intrusion of dominantly peralkaline to sub-alkaline carbonatites and intrusive silicate rocks. The latter rocks represent, with the exception of the ultramafic lamprophyres, early formed members of the complex (Andersen, 1987a, 1988). Fluids emanating from the early ijolitic intrusions caused pervasive alkali metasomatism or fenitisation of the granitic gneisses in the western half of the complex (Verschure and Maijer, 2005 and references therein). Hydrothermal veining and metasomatism overprinting the early formed fenites and their gneissic protoliths are developed in conjunction with subsequent carbonatite intrusions. It includes widespread phlogopitisation in association with abundant dykes of apatite-rich calcite-carbonatite (soevite) in the central and northern parts of the complex (Andersen, 1983, 1984, 1987b, 1989; Verschure and Maijer, 2005). The eastern half of the complex is according to Andersen and Qvale (1986) composed mainly of chlorite-ankerite ferrocarbonatites possibly representing heterogeneous pyroclastic intrusions emplaced coevally with dykes and plugs of ultramafic lamprophyres. The ferrocarbonatite is altered to a fine-grained hematite–calcite–dolomite carbonatite (rødberg) caused by oxidation of ankerite and precipitation of microscopic grains of hematite in neoformed calcite and dolomite. The formation of rødberg or carbothermal carbonatite according to the classification by Mitchell (2005) was triggered by influx of groundwater-derived hydrothermal fluids during the final stage of the ferrocarbonatite magmatism (Andersen, 1984; Andersen and Qvale, 1986). The late chlorite-bearing ferrocarbonatites, carbothermal carbonatite and carbonated gneisses in their immediate surroundings contain abundant hydrothermal veins of magnetite and hematite which were mined in the period 1652–1957 yielding a total of 1 Mt of ore (Andersen, 1983; Bugge, 1978).

*4.1.1.2. Mineralisation of Nb, Y-REE and Th.* The Søve mine produced a total of about 1 Mt of crude ore with 0.31–0.57 wt.% $Nb_2O_5$ during the period 1953–1965 (Dahlgren, 2005). Most of the ores were mined from a body of dominantly calcite-carbonatite that was followed underground from the Cappelen quarry (CQ in Fig. 2) to a depth of about 150 m (Bjørlykke and Svinndal, 1960; Sæther, 1957). Subordinate amounts of ores were also excavated from a calcite-carbonatite dyke in the Hydro quarry (HQ) and from dolomitic carbonatites in the Tufte

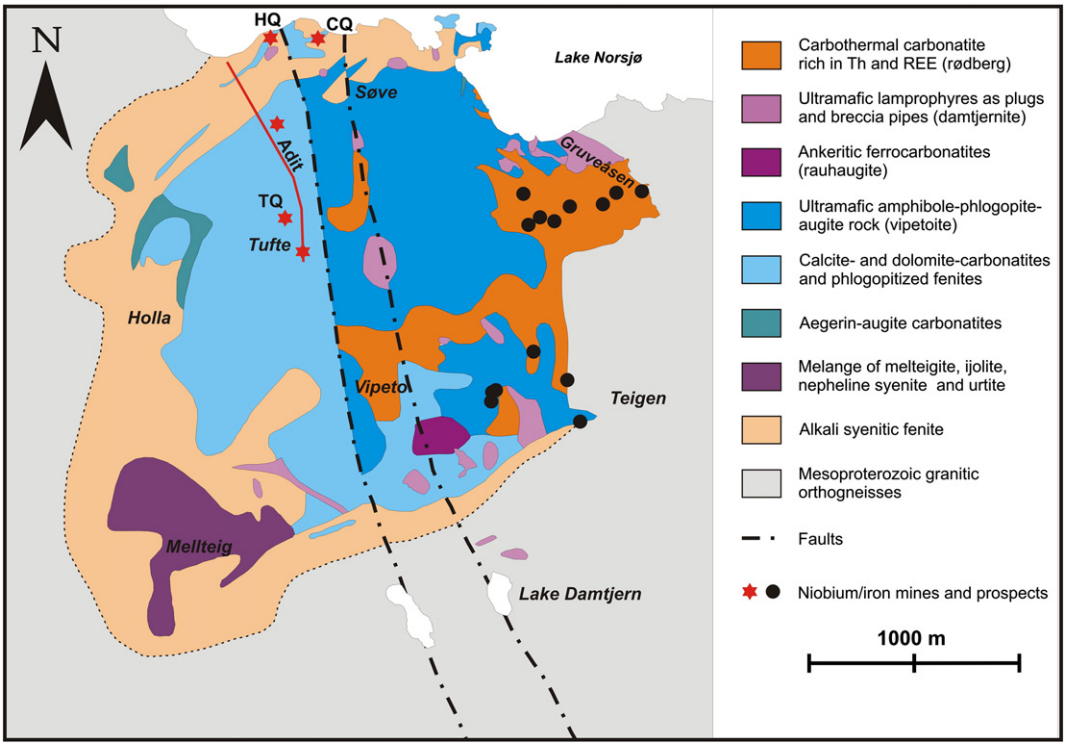


**Fig. 2.** Simplified geological map of the Fen Complex with locality names. Modified from Dahlgren (2004). Abbreviations: CQ = Cappelen quarry at Søve mine, HQ = Hydro quarry and TQ = Tufte quarry north of Tufte underground mine.

quarry and its underground workings (Fig. 2). The pyrochlore in the ores contains up 2 wt.% $ThO_2$ + REO and 2 wt.% $Ta_2O_5$ and is locally uranium-rich (Bjørlykke and Svinndal, 1960).

Presently, several companies are investigating the Fen Complex for potential resources of Y, REE and Th. The contents of these elements appear according to Bugge (1978) to successively increase from calcite-carbonatite through ankeritic ferrocarbonatite to carbothermal carbonatites, whereas the Nb content shows the opposite trend. Analyses show that the ankeritic ferrocarbonatites and carbothermal carbonatites and associated iron ores are highly enriched in REE with contents normally exceeding 0.3 wt.% TREE and with frequent analyses yielding values of 1–2 wt.% TREE (Svinndal, 1970, and references therein; Møller et al., 1980; Andersen, 1987a,b). The REE enrichment is caused by fine-grained dissemination of monazite, bastnäsite, parisite and/or synchysite (Andersen, 1986a; Lie and Østergaard, 2011a). Thorium, mainly residing in thorite, is especially enriched in the carbothermal carbonatites and associated hematite veins. They yield normally analytical values in the range 0.1–1.0 wt.% Th in contrast to 0.05–0.12 wt.% Th in the ferrocarbonatites (Lie and Østergaard, 2011a, 2011b).

*4.1.1.3. Distribution of apatite.* Presently, there exist no systematic investigations of apatite-bearing rocks in the Fen Complex. The different lithologies in the complex contain according to published major element analyses highly variable concentrations of $P_2O_5$ or apatite (Table 2). The granitic country rocks and their fenitised equivalents carry only accessory amounts of apatite. This is also the case for most of the nepheline syenites with the exception of the more melanocratic varieties which occasionally exceed 2 wt.% $P_2O_5$. A similar concentration of $P_2O_5$ is also commonly encountered in the ultramafic melteigite which according to Verschure and Maijer (2005) contains locally up to 14% apatite. The melteigite possibly representing cumulates of an ijolitic magma (Andersen, 1988) is somewhat higher in $P_2O_5$ compared with the more nepheline-rich ijolite–urtite intrusive phases and later intrusions of

**Table 2**
Summary of $P_2O_5$ analyses of different rock types in the Fen Complex. Data from 1) Verschure and Maijer (2005), 2) Brøgger (1921), 3) Andersen (1987b), and ts) this study.

| Rock type | Sample | $P_2O_5$ | | | | Source |
|---|---|---|---|---|---|---|
| | Numbers | Average | St dev | Maximum | Minimum | |
| Country rock gneisses | 15 | 0.08 | 0.06 | 0.25 | 0.02 | 1 |
| Alkali syenites | 9 | 0.71 | 0.76 | 2.34 | 0.03 | 2 |
| Ijolite–urtite | 4 | 0.98 | 0.77 | 2.12 | 0.44 | 2 |
| Nepheline pyroxenite (melteigite) | 7 | 1.86 | 0.61 | 2.58 | 0.64 | 2 |
| Aegirine calcite-carbonatite | 2 | 2.15 | 1.05 | 2.89 | 1.40 | 2 |
| Biotite–amphibole pyroxenite (vipetoite) | 2 | 3.69 | 0.25 | 3.87 | 3.51 | 2, ts |
| Biotite–calcite-carbonatite | 6 | 3.17 | 2.41 | 6.92 | 0.21 | 2, ts |
| Dolomite-carbonatite | 2 | 2.02 | 1.15 | 2.83 | 1.21 | 2, ts |
| Ankeritic ferrocarbonatite | 4 | 1.18 | 1.18 | 2.80 | 0.24 | 3 |
| Ultramafic lamprophyre | 4 | 1.01 | 0.37 | 1.36 | 0.52 | 2 |
| Carbothermal carbonatite | 7 | 2.48 | 1.76 | 5.60 | 1.25 | 2.3 |
| Hematite ore | 2 | 1.47 | 0.90 | 2.10 | 0.83 | 2.3 |

ankeritic ferrocarbonatites and associated ultramafic lamprophyres. Higher $P_2O_5$ grades are detected in the biotite–amphibole pyroxenite intrusion at Vipeto. This intrusion contains 3–4 wt.% $P_2O_5$ and characterized by up to cm long prisms of apatite and finer grained aggregates which often occur associated with abundant segregations, veinlets and narrow cross-cutting dykes and lenses of calcite- and dolomite-carbonatites. Comparable apatite-rich dykes and lenses are also found in fenites and granitic gneisses along the southern margin of the Fen Complex (Brøgger, 1921).

Most of the carbonatites in the complex are enriched in apatite which may become segregated and yield analyses exceeding 10 wt.% $P_2O_5$ (Tore Vrålstad, pers. com. 2013). Although there is a considerable spread in the analytical values for the carbonatites (Table 2), it appears from the average values that the calcite-carbonatites (3.2 wt.% $P_2O_5$) are the main carrier of apatite in the complex. The calcite-carbonatite dykes and associated dolomite-carbonatites in the Tufte–Cappelen mining area yield analytical values of up to 6.9 wt.% $P_2O_5$ (Hornig-Kjarsgaard, 1998). Ore reserve calculations by Bjørlykke (1953) prior to the opening of the Søve mine gave an estimate of 1.4 Mt with 0.24 wt.% $Nb_2O_5$ and 3.21 wt.% $P_2O_5$ in the Cappelen and Hydro ore bodies. The Tufte deposit was regarded to be higher in apatite (~4.6 wt.% $P_2O_5$), but lower in niobium. The apatite in the carbonatites occurs as 2–5 mm long prismatic phenocrysts which often have recrystallised to granular aggregates of equidimensional grains (0.1–0.2 mm; Andersen, 1986a). In the Tufte area there occur a number of apatite-rich lens-shaped bodies varying in composition from almost carbonate-free apatite–phlogopite–amphibole–magnetite rocks to apatite-rich calcite- and dolomite-carbonatites (Andersen, 1986b). On the basis of fluid inclusion studies and intergrowth textures Andersen (1986b, 1987a, 1988) advocated that the apatite represent an early liquidus mineral which largely crystallised prior to the final emplacement of the carbonatite magma. The carbonate-poor and apatite-rich rocks probably formed as cumulates from the carbonatite magma in the middle crust and transported to their present position by the ascending carbonatite magma (Andersen, 1986b, 1987a). One sample of these apatite-rich cumulates shows a modal composition of 29% apatite, 6% titanomagnetite, 2% pyrochlore and 62% calcite (Hornig-Kjarsgaard, 1998).

The ankeritic ferrocarbonatite is lower in apatite than the other carbonatite types (Table 2) and carries normally 1–2% modal apatite, locally rising to 5–10% (Sæther, 1957). The carbothermal carbonatites show a similar spread in analytical values as the calcite-carbonatites, but with a lower average (2.4 wt.% $P_2O_5$). The hydrothermal hematite ores worked by the Fen iron mines contained according to Bugge (1978) an average of 1.05wt.% $P_2O_5$. Three apatite concentrates from the calcite-carbonatites yield TREE in the range of 3752–5220 ppm and 164–288 ppm Y, whereas one apatite concentrate extracted from dolomite-carbonatite gave 5143 ppm TREE and 199 ppm Y (Hornig-Kjarsgaard, 1998).

A proper evaluation of the apatite resources in the Fen Complex has to await more systematic sampling. Presently it appears that apatite in the carbonatites may represent a potential by-product if exploitable Nb and REE + Y deposits are defined in the future.

### 4.1.2. Alkaline complexes of the Seiland Igneous Province

*4.1.2.1. Geological outline.* The Seiland Igneous Province (SIP) is part of the Kalak Nappe Complex in the Middle Allochthon of the Caledonides in Northern Norway (Roberts and Gee, 1985). The intrusions constituting the SIP cover an area of more than 5000 km$^2$. They were emplaced into arenaceous meta-sedimentary rocks containing pelitic to semi-pelitic units with some interlayered marbles (Roberts, 1973). Most of the plutonic rocks and their wall rocks are affected by two tectonothermal events (D1 and D2) which mainly occurred under amphibolite to granulite facies conditions (Elvevold et al., 1994; Robins, 1996, and references therein). The bulk of the various intrusions of the SIP was emplaced in the Ediacaran (570–560 Ma) with some of the late nepheline syenite dykes spilling into early Cambrian (530–520 Ma) (Pedersen et al, 1989; Roberts et al., 2010). The SIP comprises a wide spectrum of magmas. The early stage intrusions according to Robins (1996) comprise sub-alkaline gabbros of calc-alkaline affinity that are intruded by late diorites, monzonites and granitoids in their interior (Fig. 3). The intermediate stage is the most voluminous. It consists of layered massifs of gabbronorites and norites (some of them showing tholeiitic trends) that are followed by emplacement of syenogabbros with magma composition transitional to alkali basalts. Subsequent intrusions are represented by layered olivine gabbros often carrying associated pegmatitic gabbros (Tappeluft) and ultramafic massifs derived from more alkaline magmas (alkali olivine basaltic or alkali picritic). The late stage intrusions comprise mainly strongly alkaline rocks (syenites, nepheline syenites and carbonatites) derived from nephelinitic magmas (Robins, 1996). The rocks constituting the phosphorous alkaline complexes at Lillebukt, Breivikbotn, and Pollen include alkaline nepheline syenites, hornblende clinopyroxenites and carbonatites with associated envelopes of mafic-ultramafic fenites. The miascitic chemistry of the alkaline rocks that was identified by Barth (1927) may have an indirect influence on the characteristically low contents of REE and high field strength elements in these rocks (Heier, 1961). The mafic–ultramafic fenites which represent metasomatic alteration of the gabbroic wall rocks are very heterogeneous in composition and contain frequently nebulitic remnants of the protolith. It is a coarse-grained ultramafic rock composed of variable proportions of amphibole, aegirine–augite, biotite, apatite and calcite. The

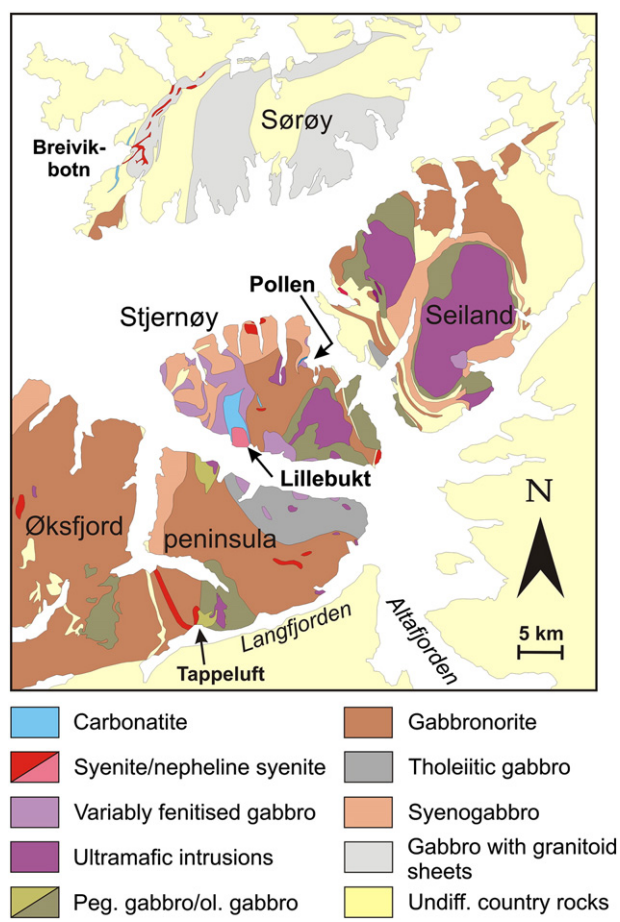


**Fig. 3.** Simplified geological map of the Seiland Igneous Province showing the location of the apatite-bearing pegmatitic gabbro and alkaline complexes. Most of the gabbro massifs show development of igneous layering, The map is compiled from Roberts (1973), Robins and Gardner (1974), Robins (1982), Bennett et al. (1986), Mørk and Stabel (1990) and Elvevold et al. (1994).

fenites are enriched in P, C, Zr, Sr, Nb, Ba, LREE, Ti, Fe, Ca, K and Mn and depleted in Si, Al and Na relative to the composition of the gabbroic protolith (Robins and Tysseland, 1983). The overall rock association, and geochemistry indicate formation of SIP in a continental rift during crustal extension (Roberts et al., 2010).

*4.1.2.2. Apatite distribution in selected intrusions.* Apatite represents an accessory mineral in most of the intrusions, but is especially enriched in those derived from alkali basaltic and nephelinitic magmas, including the Tappeluft, Breivikbotn, Pollen and Lillebukt intrusions which have been explored in some detail by a number of companies. The Tappeluft pegmatitic gabbro (Fig. 3; Mørk and Stabel, 1990) which was sampled by Norsk Hydro contains an average of 1.88 wt.% $P_2O_5$ and a maximum of 4.29 wt.% $P_2O_5$ (Aggerholm and Parr, 1984). The Breivikbotn alkaline complex yields modal apatite contents in the following ranges for the different rocks of the complex: Nepheline syenites: 0.1–0.5%; aegerine–augite pyroxenites: 0.4–7.7%; melanocratic syenites: 0.5–8.7%; syenites: 0.2–2.7% and carbonatites: 0.3–6.4% (Sturt and Ramsay, 1965).

The Lillebukt Complex (no. 1) is the only one that has been mapped in detail by MSc students from the University of Bergen and explored by Elkem, Yara International and NGU. It is situated on the southern central part of the island Stjernøy (Fig. 3) and covers an area of about 13 km$^2$ (Gautneb and Ihlen, 2009; Skogen, 1980b). It is the largest of the alkaline complexes within the SIP and is hosted by layered metagabbros belonging to the intermediate stage of plutonic activity in the province. The development of the complex started with the emplacement of hornblende clinopyroxenite dykes followed by intrusions of monzonites, syenites, nepheline syenites, carbonatites and late nepheline syenite pegmatites (Fig. 4). Mafic fenites derived from the layered gabbros and felsic fenites formed by metasomatism of early syenites and monzonites in the south constitute together a 500–1000 m wide zone around the central carbonatite intrusion.

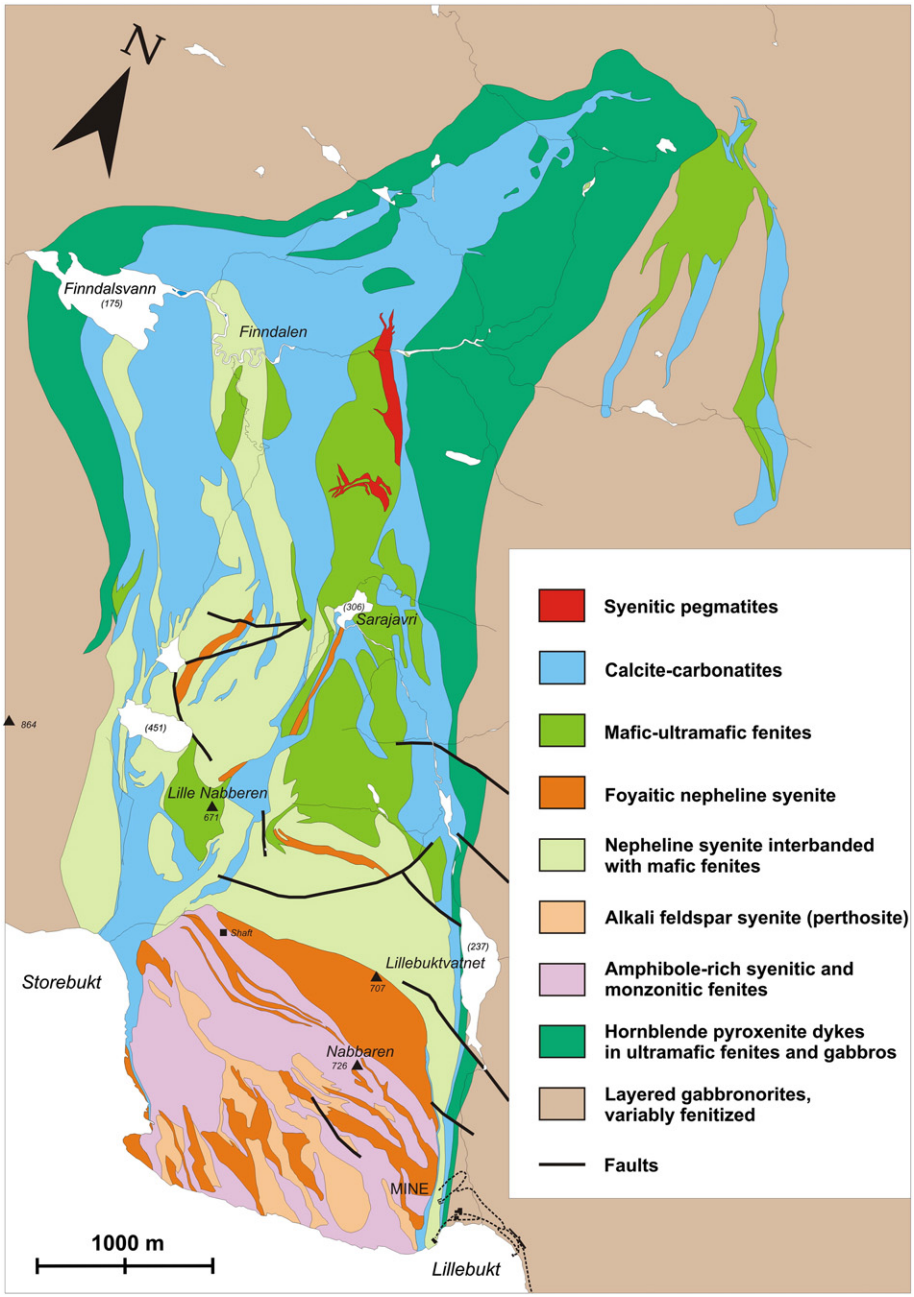


**Fig. 4.** Simplified geological map of the Lillebukt Complex. Redrawn from compilation made by Bruland, T., Kjøsnes, K., Mjelde, Ø., Skogen, J.H., Strand, T., Robins, B., 1981, University of Bergen.

The main apatite-bearing rock types are hornblende clinopyroxenite dykes and calcite-carbonatites. The former dykes occur abundantly in the mafic fenites and gabbros along the northern and eastern margins of the complex where they form a 50–600 m wide and 11 km long belt of sub-parallel dykes separated by screens of ultramafic fenites constituting about 40% of the rocks. Individual dykes are generally 50–100 cm wide with a maximum width of 10 m. They consist of aluminous titanian salite, magnesian hastingsite and apatite together with commonly sub-ordinate ilmenite and ilmenomagnetite, as well as minor hercynitic spinel and calcite (Robins, 1985). These steeply-dipping coarse-grained to pegmatitic dykes commonly show an inward directed growth of up to 50 cm long crystals of clinopyroxene and hornblende forming comb structures with interstitial aggregates of coarse-grained apatite which is locally developed in up to 10 cm large skeletal crystals. Some of the dykes are unusually apatite-rich, often with cores containing up to 50 vol.% apatite and Fe–Ti oxides (Robins, 1985).

The mineralogy and petrochemistry of the carbonatites were investigated by Strand (1981) who revealed that the carbonatites of the complex represent calcitic silicocarbonatite with about 40% of strontian calcite. The main minerals comprise calcite, biotite, alkali hastingsite, apatite, ilmenite and titanomagnetite and occur together with minor alkali feldspar and nepheline. Apatite occurs as evenly distributed mm-sized prisms (Fig. 5a). Fe–Ti oxides are common locally. The carbonatite has developed a crude banding defined by variable proportions and alignments of mafic minerals that are the result of mechanical redistribution and recrystallization during post-magmatic deformation and metamorphism (Skogen, 1980a; Strand, 1981).

A total of 330 grab and percussion-drilling samples have been collected from the carbonatites and hornblende-clinopyroxenite dykes. The latter includes probably also samples of the thin screens of ultramafic fenites which generally are low in apatite. The carbonatites (218 analyses) show an average of 2.33 wt.% $P_2O_5$ with a maximum of 6.45 wt.% $P_2O_5$. 23 of these samples contain more than 6 wt.% $P_2O_5$. The hornblende clinopyroxenites (56 analyses) yield an average of 2.35 wt.% $P_2O_5$ which is similar to the average for the carbonatites. 4 of these analyses gave values in excess of 8.00 wt.% $P_2O_5$ with a maximum of 13.49 wt.% $P_2O_5$. The average content of apatite in all samples is 5.6 wt.% apatite. In well-exposed and densely sampled areas of

**Fig. 5.** Macroscopic features of the different types of apatite ores. a) Apatite-bearing biotite calcite-carbonatite of the Lillebukt Complex (length of match is 44 mm), b) ultrapotassic coarse-grained biotite pyroxenite in the Misværdal Complex with interstitial white alkali feldspar aggregates and light grey acicular apatite (diameter of coin is 26 mm), c) layered apatite–Fe–Ti oxide ore of MCU IV in the Bjerkreim–Sokndal Layered Intrusion of the RAP (length of hammer is 0.7 m), d) close-up of nelsonite (black) breccia-dyke at Nordre Følstad in the LVMC containing fragments of the wall rocks comprising charnockite and mangerite dykes in fine-grained felsic granulites (length of hammer is 0.5 m), and e) patchy dark apatite–Fe–Ti oxide ore in mangerite at Grindvika in the LVMC (length of magnet pen is 13 cm),.

about 300 m × 300 m in the carbonatite and clinopyroxenite dykes yield averages of 3.00 wt.% $P_2O_5$ and 2.93 wt.% $P_2O_5$, respectively. Analyses of hand-picked coarse-grained crystals show that the apatite from the carbonatite contains 5601 ppm TREE and 288 ppm Y that are higher than apatite from a hornblende clinopyroxenite dyke with 3562 ppm TREE and 335 ppm Y (Table 3; Gautneb, 2010). However, one of the hand-picked apatite crystals from the carbonatite contained 11,084 ppm TREE and 5045 ppm Ce which may suggest intergrowth with monazite.

The average grades of 3.0 wt.% $P_2O_5$ in both carbonatites and clinopyroxenites suggest that the Lillebukt complex is too low-grade to represent any important resource of apatite. In addition, the low to moderate contents of TREE + Y in the apatite comparable to those in the Fen alkaline complex give probably no extra value to the deposit. This resource estimate appears also to be the case for the Tappeluft, Breivikbotn and Pollen deposits.

*4.1.3. The Misværdal Complex*

The Misværdal Complex (MC, no. 7 in Fig. 1) was discovered by Farrow (1974) in conjunction with regional bedrock mapping when the enrichment of apatite in the pyroxenites also was noted. However, apatite as a potential mineral resource was first recognized in 2006, i.e. more than 30 years later, by Nordland Mineral and NGU. The text below is largely based on unpublished results of subsequent bedrock mapping and lithochemical investigations conducted by the first author mainly in the period 2008–2010 (Ihlen, 2009; Ihlen and Furuhaug, 2012).

*4.1.3.1. Geological outline.* The MC comprises multiple intrusions of clinopyroxenites forming two bodies measuring 6 $km^2$ and 2 $km^2$, respectively (Fig. 6). They intrude various types of mica schists, marbles and migmatitic paragneisses that are also truncated by dykes and batholithic bodies of granites, granodiorites and tonalites (Farrow, 1974; Solli et al., 1992; Tørudbakken and Brattli, 1985). One of these granites yields a Rb–Sr age of 440 ± 30 Ma which falls within the age range of other comparable calc-alkaline to alkali-calcic granitic batholiths of late Ordovician and Silurian age found elsewhere in the Uppermost Allochthon of northern Norway (Tørudbakken and Brattli, 1985; Barnes et al., 2011, and references therein). Contact relationships between the MC and the granites, including mingling structures indicate that they were emplaced roughly contemporaneously.

The emplacement of the MC post-dates sillimanite- and kyanite-grade peak metamorphism and associated development of penetrative foliation in the wall rocks (Solli et al., 1992; Tørudbakken and Brattli, 1985). Although the clinopyroxenites appear to be only weakly deformed in most outcrops, they have lost most of their primary igneous textures (especially the fine- to medium-grained types) in conjunction with greenschist facies retrogradation associated with late development of narrow ductile shear zones and high-strain zones.

The pyroxenites are mainly composed of augitic clinopyroxene (>70 vol.%) and variable proportions of biotite, mesoperthitic alkali feldspar and apatite. Four types of clinopyroxenites can be distinguished (Fig. 6). Major element analyses reveal ultrapotassic bulk compositions (i.e. molar ratio of $K_2O/Na_2O > 3$) for most types due to high contents of biotite and alkali feldspar. The most voluminous of these is the fine- to medium-grained biotite clinopyroxenites (termed fine-grained pyroxenites in the text below) which even on an outcrop scale may grade into a number of sub-types. One of these are characterized by dense dissemination and irregular segregations, lenses and veinlets of coarse-grained, often monomineralic aggregates of biotite. This glimmeritic type is frequently rich in apatite especially along the gradational contacts with coarse-grained to pegmatitic segregations which are composed of acicular clinopyroxene crystals (1–10 cm long) in a matrix of up to 80% mesoperthitic alkali feldspar together with apatite and biotite. These up to several tens of metres sized segregations, possibly representing residual liquids, are similar in composition and appearance to thin dykes and major intrusive bodies of coarse-grained apatite–biotite–alkali feldspar clinopyroxenites (Fig. 5b; termed as coarse-grained pyroxenites in the text below) cutting the fine-grained pyroxenites in different directions (Fig. 6). The coarse-grained pyroxenites are commonly only weakly deformed and retrograded and have largely retained their igneous texture and mineralogy. In some of them alkali feldspar is missing and this sub-type is generally rich in biotite (20–60 vol.%), but low in apatite. The biotite-rich rocks are probably of metasomatic origin assumed to be caused by volatiles expelled from crystallising magmas of coarse-grained pyroxenites or from carbonatites at depth. All of the clinopyroxenites are cross-cut by abundant thin dykes of coarse-grained to pegmatitic alkali feldspar syenites and monzonites, as well as some small dykes of calcite-carbonatites. The fine-grained pyroxenites often form globulitic mingling structures with the monzonites that are commonly encountered in the southern satellite intrusion where a number of intermediate rock types are developed.

The mineral assemblage of the clinopyroxenites (modal and normative) is characterized by the absence of foids, indicating that the magmas were silica saturated. Subordinate biotite-free clinopyroxenites have a sub-alkaline bulk composition whereas those containing biotite and/or alkali feldspar are alkaline and ultrapotassic. The composition of the rocks fits none of the common classification schemes for mafic–ultramafic igneous rocks given by Le Maitre (2002). The silica-saturation, the frequent mingling structures with felsic intrusions and low contents of $TiO_2 = 0.99 \pm 0.28$ (normally titanite, rarely ilmenomagnetite) suggest a link to the temporally associated calk-alkaline and alkali-calcic granitic plutons. One possibility is that the rocks formed by differentiation of a magma generated by mixing of granitic, and phosphorus-rich lamproitic or shoshonitic magmas.

*4.1.3.2. Apatite distribution.* The fine-grained pyroxenites contain normally about 5 vol.% apatite which is mainly found as equidimensional interstitial grains (0.1–0.5 mm) in the recrystallised granular matrix of clinopyroxene. It is occasionally also seen as inclusions in biotite and in larger crystals of clinopyroxene. The coarse-grained pyroxenites which are the main carrier of potential apatite resources in the MC

**Table 3**
ICP-MS analyses of REE, Y and Th in apatite concentrates from the Lillebukt, Misværdal, Nordre (N) Følstad, Grindvika, Kodal and Rossavika deposits. Abbreviations: bio. = biotite, carb. = carbonatite, cgr. = coarse-grained, fgr. = fine-grained, hbl. = hornblende, and h.w. = hanging-wall zone of the massive ore bodies.

| DEPOSIT | HOST ROCK | La | Ce | Pr | Nd | Sm | Eu | Gd | Tb | Dy | Ho | Er | Tm | Yb | Lu | TREE | Y | Th |
|---|---|---|---|---|---|---|---|---|---|---|---|---|---|---|---|---|---|---|
| Lillebukt | Bio. calcite-carb. | 1052.7 | 2501.2 | 295.3 | 1195.9 | 194.9 | 57.8 | 158.1 | 18.0 | 78.0 | 11.1 | 23.2 | 2.4 | 11.4 | 1.3 | 5601.2 | 287.8 | 0.5 |
| | Bio. calcite-carb. | 2258.3 | 5045.5 | 578.6 | 2255.3 | 330.9 | 96.0 | 258.3 | 29.2 | 128.3 | 18.6 | 38.1 | 4.0 | 20.8 | 2.3 | 11,064.1 | 485.6 | 0.2 |
| | Hbl. pyroxenite | 842.5 | 1648.5 | 166.7 | 676.8 | 82.4 | 21.5 | 62.3 | 6.7 | 32.5 | | 11.8 | 1.2 | 7.7 | 1.1 | 3561.7 | 131.8 | 50.2 |
| Misværdal | Fgr. pyroxenite | 486.5 | 1506.2 | 248.5 | 1277.1 | 269.6 | 59.8 | 214.9 | 23.7 | 105.9 | 15.9 | 32.6 | 4.0 | 22.6 | 2.7 | 4270.0 | 425.9 | 124.7 |
| | Cgr. pyroxenite | 658.6 | 1567.9 | 233.4 | 1074.9 | 208.7 | 45.8 | 160.7 | 16.1 | 67.6 | 8.7 | 16.9 | 2.1 | 12.0 | 1.4 | 4074.7 | 253.0 | 62.8 |
| | Cgr. pyroxenite | 456.3 | 1457.7 | 226.6 | 1112.6 | 231.0 | 50.2 | 183.1 | 20.0 | 85.0 | 12.1 | 26.1 | 3.1 | 16.7 | 2.3 | 3882.9 | 334.8 | 60.1 |
| N. Følstad | Nelsonite | 651.6 | 1248.9 | 236.9 | 1224.9 | 286.5 | 10.4 | 304.7 | 45.4 | 279.2 | 52.9 | 138.8 | 18.9 | 103.3 | 13.2 | 4615.6 | 1394.0 | 51.1 |
| Grindvika | Pyroxenitic ore | 940.3 | 2411.3 | 355.4 | 1668.8 | 313.0 | 33.7 | 274.1 | 33.3 | 170.3 | 29.9 | 71.8 | 8.6 | 47.4 | 6.1 | 6364.0 | 818.4 | 9.5 |
| Kodal | Pyroxenitic ore, h.w. | 1554.6 | 3381.8 | 424.2 | 1729.1 | 269.3 | 52.5 | 229.7 | 26.4 | 129.5 | 23.0 | 57.0 | 6.9 | 39.1 | 5.1 | 7928.1 | 630.1 | 44.6 |
| | Pyroxenitic ore, h.w. | 2048.2 | 4360.3 | 524.6 | 2059.3 | 314.5 | 49.0 | 267.8 | 30.4 | 152.2 | 26.6 | 64.4 | 8.1 | 46.6 | 6.0 | 9957.8 | 737.4 | 44.2 |
| Rossavika | Carbonate lens | 744.4 | 1611.9 | 219.7 | 905.6 | 123.0 | 28.7 | 90.2 | 8.7 | 39.5 | 6.0 | 13.9 | 1.8 | 10.9 | 1.4 | 3805.6 | 183.7 | 22.7 |

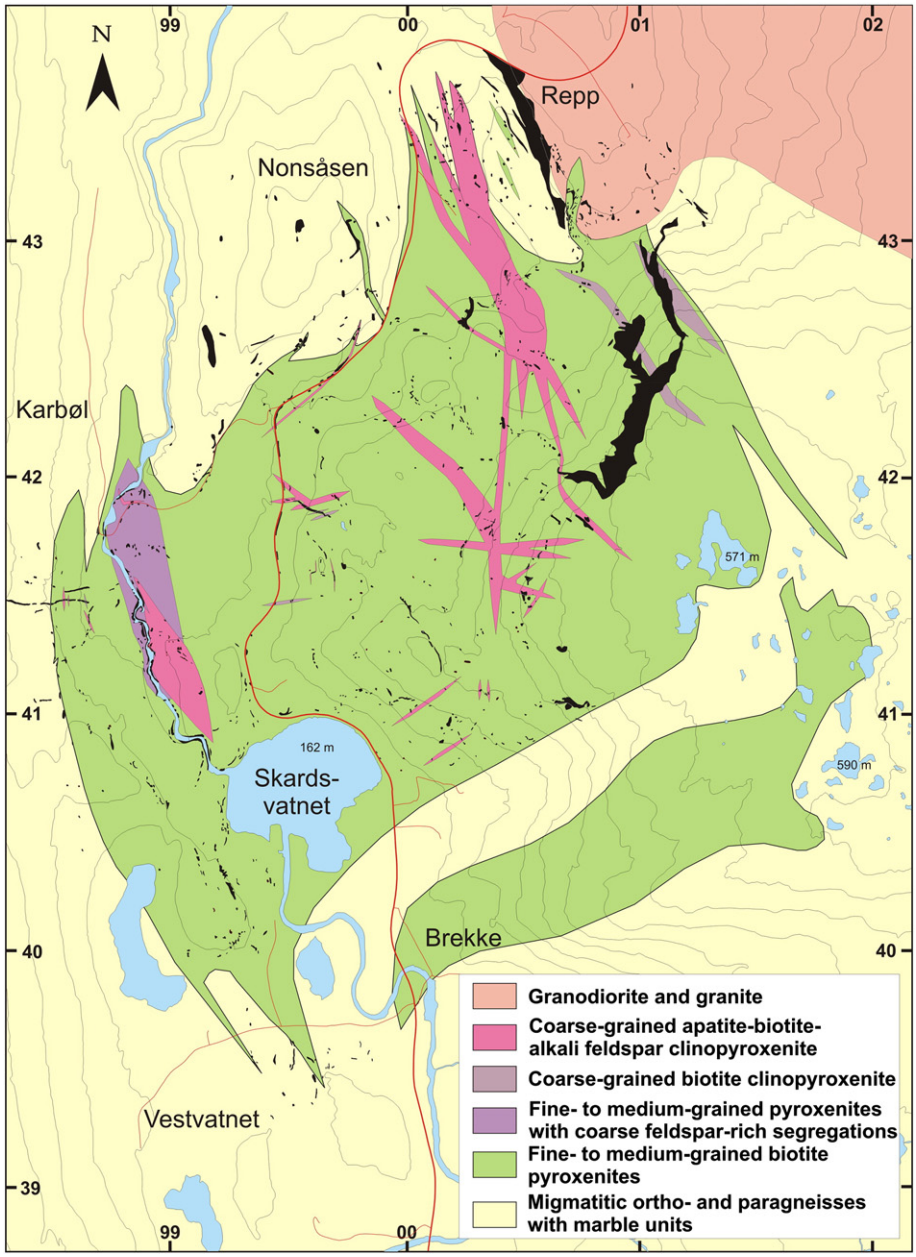


**Fig. 6.** Simplified geological map of the Misværdal Complex based on mapping by the first author. Black areas and dots represent outcrops. Numbers on the frame are kilometre units for UTM coordinates (EUREF 89) in grid zone 33 W. 50 m altitude contours. Lake Skardsvatnet is situated at 162 m above sea level. Roads shown as red lines.

contain apatite as 1–30 mm long acicular crystals which frequently have recrystallised to needle-shaped granular aggregates of fine-grained apatite. The apatite represents an early liquidus mineral which locally segregates to form cumulates with interstitial biotite and alkali feldspar. The cumulus-forming process may explain the very uneven distribution of apatite between outcrops and within individual outcrops (Ihlen and Furuhaug, 2012). The total average for 283 clinopyroxenite samples is 2.38 wt.% $P_2O_5$. The highest values are found associated with the coarse-grained pyroxenite segregations and their intrusive counterparts which both contain averages of 2.5 wt.% $P_2O_5$ or about 6 wt.% apatite. In spite of these rather low values, presently of no economic interest, it has been possible so far to define a zone, 200 m wide and more than 650 m long, in the western part of the complex where sampled outcrops of coarse-grained pyroxenite yield an average of 4.1 wt.% $P_2O_5$ or about 10 wt.% apatite.

Laser ablation ICP-MS analyses of single grains of apatite in polished sections of coarse-grained pyroxenites yield TREE in the range of 1243–11,180 ppm with averages in the range of 4150–6353 ppm TREE for the individual sections (Table 4). The large variations in TREE may be caused by the retrograde formation of allanite frequently forming micro-networks in the apatite aggregates and possibly extracting variable amounts of REE from the apatite. ICP-MS analyses of apatite concentrates from a fine-grained pyroxenite gave 4270 ppm TREE, whereas concentrates from coarse-grained pyroxenites yield values in the range of 3883–4075 ppm TREE (Table 3). The latter range is considerably lower than the averages of the LA-ICP-MS analyses from the same samples, i.e. 3883 ppm TREE (ICP-MS) versus 5581 ppm TREE (LA-ICP-MS). Such interlaboratory and intermethod differences are not uncommon. Thus, a direct comparison of analytical values for apatite should be made with caution as long as the analytical method is not known. However, both methods yield high average contents of Th reaching 100 ppm in some samples which is about the double of the amount accepted for raw materials to NPK-fertilizers. This is the main obstacle regarding the utilization of apatite from the MC

**Table 4**
LA-ICP-MS analyses of apatite grains in polished sections from the Misværdal Complex, the Bjerkreim–Sokndal Layered Intrusion and the Kodal deposit. 5–14 single grains of apatite in each section were analysed. Averages of REE, Y and Th in apatite per polished section are given. All of the single-grain analyses are available upon request to the corresponding author.

| DEPOSIT | HOST ROCK | La | Ce | Pr | Nd | Sm | Eu | Gd | Tb | Dy | Ho | Er | Tm | Yb | Lu | Σ REE | Th |
|---|---|---|---|---|---|---|---|---|---|---|---|---|---|---|---|---|---|
| | Coarse-grained pyroxenite | 530.4 | 1910.1 | 237.5 | 933.4 | 213.8 | 50.4 | 152.9 | 16.0 | 65.1 | 9.3 | 18.3 | 1.9 | 10.0 | 1.2 | 4150.5 | 70.5 |
| Misværdal | Coarse-grained pyroxenite | 737.3 | 2654.2 | 357.3 | 1394.0 | 309.5 | 73.7 | 215.4 | 23.4 | 94.3 | 13.8 | 26.2 | 2.7 | 14.3 | 1.7 | 5917.7 | 99.9 |
| | Coarse-grained pyroxenite | 989.4 | 2978.8 | 353.2 | 1340.5 | 283.3 | 65.5 | 194.8 | 20.4 | 80.2 | 11.4 | 21.2 | 2.2 | 11.3 | 1.3 | 6353.2 | 95.4 |
| | Coarse-grained pyroxenite | 745.1 | 2551.4 | 331.4 | 1294.2 | 271.5 | 62.5 | 182.3 | 19.1 | 76.2 | 11.2 | 21.0 | 2.2 | 11.9 | 1.5 | 5581.3 | 60.5 |
| Bjerkreim– | Apatite–Fe–Ti ore, Megacycle I | 164.5 | 494.4 | 78.0 | 356.5 | 91.8 | 26.2 | 91.1 | 10.7 | 53.3 | 9.3 | 20.4 | 2.0 | 10.7 | 1.4 | 1410.3 | 1.6 |
| Sokndal | Apatite–Fe–Ti ore, Megacycle III | 179.6 | 558.3 | 81.2 | 367.1 | 91.5 | 23.4 | 86.1 | 10.1 | 48.6 | 8.2 | 17.4 | 1.8 | 9.1 | 1.0 | 1483.5 | 2.4 |
| Layered | Apatite–Fe–Ti ore, Megacycle IV | 178.6 | 512.0 | 76.8 | 349.9 | 86.7 | 21.5 | 82.2 | 9.6 | 46.7 | 7.9 | 16.9 | 1.7 | 8.8 | 1.0 | 1400.3 | 2.9 |
| Intrusion | Apatite–Fe–Ti ore, Megacycle IV | 189.3 | 571.5 | 84.2 | 345.6 | 86.3 | 21.7 | 83.1 | 9.7 | 46.7 | 7.9 | 16.8 | 1.7 | 8.8 | 1.1 | 1474.4 | 6.7 |
| Kodal | Monzonite, hanging wall | 1286.7 | 2578.5 | 249.0 | 818.8 | 131.1 | 22.4 | 108.7 | 12.6 | 61.9 | 11.9 | 27.5 | 3.3 | 19.4 | 2.8 | 5334.6 | 36.6 |
| | Patchy ore, hanging wall | 1625.2 | 3693.4 | 374.4 | 1269.7 | 215.5 | 25.2 | 170.4 | 19.9 | 98.6 | 18.2 | 41.6 | 4.8 | 27.8 | 3.7 | 7588.4 | 51.8 |
| | Ore zone, upper part | 1601.2 | 4346.5 | 483.6 | 1690.7 | 301.3 | 49.9 | 223.9 | 27.5 | 138.7 | 24.7 | 58.3 | 6.7 | 38.0 | 4.7 | 8995.8 | 25.8 |
| | Ore zone, central part | 2233.2 | 5352.9 | 575.2 | 1910.9 | 323.3 | 58.0 | 235.9 | 28.8 | 140.9 | 24.9 | 58.5 | 6.6 | 36.1 | 4.5 | 10,989.5 | 27.3 |
| | Ore zone, lower part | 1787.8 | 4126.4 | 474.4 | 1674.9 | 296.5 | 62.6 | 230.4 | 27.1 | 132.4 | 23.3 | 49.9 | 5.6 | 31.5 | 3.8 | 8926.6 | 30.4 |
| | Patchy ore, footwall | 2456.5 | 4521.9 | 462.1 | 1601.7 | 272.0 | 25.5 | 230.2 | 27.2 | 136.5 | 25.9 | 58.1 | 7.1 | 43.6 | 6.4 | 9874.8 | 70.7 |
| | Monzonite, foot wall | 2012.1 | 3760.9 | 377.5 | 1254.4 | 200.9 | 28.4 | 164.7 | 18.8 | 92.5 | 17.4 | 41.1 | 4.8 | 27.6 | 4.0 | 8005.1 | 57.7 |

since the present use and consumption of Th are very limited. Thus, further exploration for potential resources of apatite in the heavily covered MC has to await new developments in the processing and use of Th.

### 4.2. Deposits in massif-type anorthosite complexes

#### 4.2.1. The Rogaland Anorthosite Province

The Rogaland Anorthosite Province (RAP) is one of a kind in the Fennoscandian Shield. It is located along the coast of southwest Norway where it covers an on-shore area of roughly 1750 km$^2$ (Fig. 7). The RAP comprises a suite of intrusions including massif-type anorthosites, leuconorites, norites, jotunites, mangerites and charnockites. It represents one of the latest magmatic events of the Sveconorwegian orogeny and according to Schärer et al. (1996) and Vander Auwera et al. (2011) was emplaced during two short lived plutonic events at 933–929 Ma and 920–916 Ma. The exposed gneissic country rocks comprise Mesoproterozoic (1520 Ma and younger) metavolcanic, metaplutonic and metasedimentary lithologies which are affected by long-standing granulite facies metamorphism starting at about 1030 Ma (Bingen et al., 2008, and references herein).

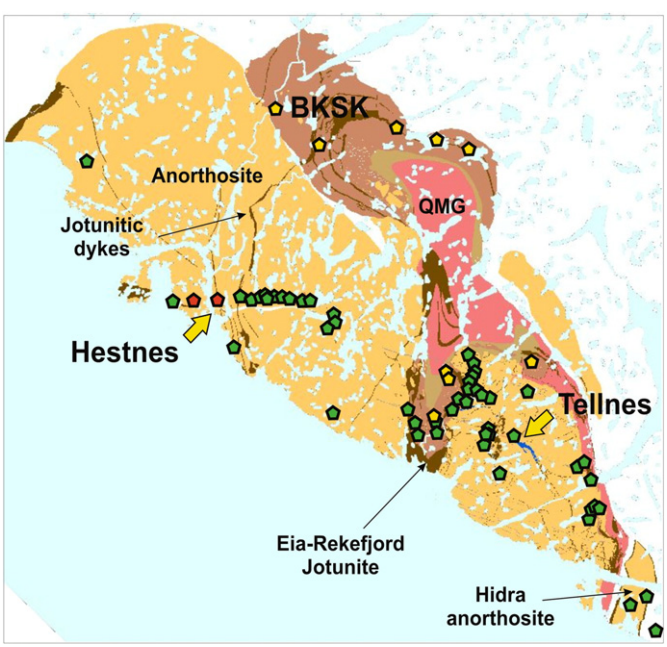


**Fig. 7.** Simplified geological map of the Rogaland Anorthosite Province showing the intrusions mentioned in the text together with the location of Fe–Ti oxide deposits (green) and apatite–Fe–Ti oxide deposits (red).

The RAP is dominated volumetrically by a number of massif-type anorthosite plutons consisting of more or less monotonous anorthosites or leuconorites. The somewhat younger Bjerkreim–Sokndal Layered Intrusion (BKSK) measuring 230 km$^2$, is considered to be the largest layered intrusion in Western Europe, and comprises cumulates fractionated from a jotunitic magma (Duchesne and Hertogen, 1988; Robins et al., 1997). The last plutonic event terminating the magmatic activity in the RAP comprises charnockitic to mangeritic intrusions and dykes of jotunitic to noritic compositions — including the world class Tellnes ilmenite deposit (Schärer et al., 1996; Vander Auwera et al., 2011).

Genetic models tend to involve primitive jotunitic to high alumina basaltic parental melts subjected to a polybaric differentiation history to account for all the various units in the province (Charlier et al., 2010; Duchesne and Hertogen, 1988; Longhi et al., 1999; Robins et al., 1997). A lower crustal source for these magmas has been advocated by a number of authors. (Duchesne et al., 1999; Longhi, 2005; Longhi et al., 1999; Schiellerup et al., 2000; Vander Auwera et al., 2011).

Apatite is present in most intermediary and evolved lithologies such as titaniferous jotunites and gabbronorites. Jotunite dykes of variable size and form transect both the anorthosite massifs and other major intrusions, such as the BKSK. They represent the youngest intrusive event in the province. The Lomland and Varberg dykes intersecting the Egersund–Ogna anorthosite massif are reported to contain 2.99 wt.% $P_2O_5$ and 4.05 wt.% $P_2O_5$, respectively (Duchesne and Schiellerup, 2001). Jotunite enriched in phosphorus also occurs in a more primitive form as marginal chills to both the BKSK and the Hidra massif anorthosite, as well as in marginal rocks of the Tellnes intrusion. Apatite-bearing gabbronorites found higher in the stratigraphy of the BKSK are invariably more evolved cumulates saturated in multiple minerals.

The RAP also contains a large variety and number of Fe–Ti deposits and occurrences (Schiellerup et al., 2003) and some of these are also enriched in apatite (e.g. Hestenes; Fig. 7). The apatite-bearing types include narrow nelsonite dykes and lenses intersecting the northern sheared margin of the Håland–Helleren anorthosite massif (Fig. 7). The nelsonite dykes are almost devoid of silicates and consist of fairly equal amounts of apatite and Fe–Ti oxides (Duchesne and Schiellerup, 2001).

*4.2.1.1. Deposits in the Bjerkreim–Sokndal Layered Intrusion.* The most prominent of the apatite deposits is hosted by the Bjerkreim–Sokndal Layered Intrusion (BKSK). This intrusion contains a more than 7000 m thick Layered Series consisting of anorthosite, leuconorite, leucotroctolite, norite and gabbronorite (e.g., Wilson et al., 1996; Fig. 8). The Layered Series is overlain by a jotunitic Transition Zone and finally capped by increasingly monotonous mangerites, quartz-mangerites and charnockites where apatite mineralisation appears to be missing. Fine to medium grained jotunitic rocks found along the margins of the intrusion have

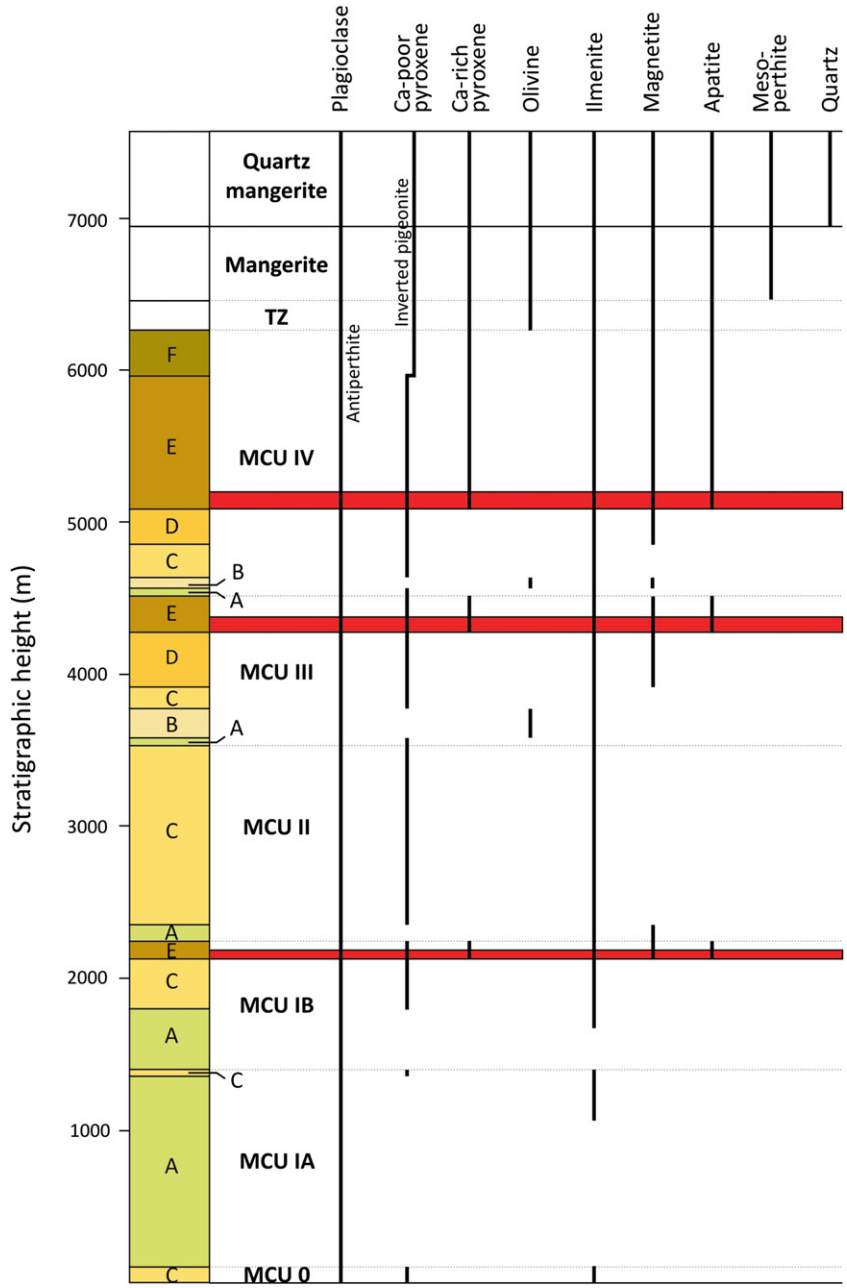


**Fig. 8.** Generalised zone stratigraphy and phase layering of the Layered Series in the Bjerkreim–Sokndal Layered Intrusion in the RAP.

been interpreted as marginal chills and suggest a Fe- and Ti-enriched, relatively Ca-poor basaltic parental magma (Duchesne and Hertogen, 1988; Robins et al., 1997). The $P_2O_5$ content of the fine grained marginal rocks is between 0.6 and 1.1 wt.%.

The intrusion has been deformed into a roughly north–south elongated syncline or trough, at least partly due to gravitational subsidence of the core of the intrusion at a late- to post-magmatic stage (Bolle et al., 2002; Paludan et al., 1994). The cumulate sequence is thickest along the south plunging axis of the northern Bjerkreim-lobe.

The Layered Series are organised into 6 megacyclic units (MCU 0, IA, IB, II, III, and IV) each resulting from recharge of relatively primitive magma. Phase layering is distinct within the megacyclic units reflecting the general order of crystallisation: plagioclase (±olivine), ilmenite, orthopyroxene, magnetite, clinopyroxene and apatite. In addition magnetite is a cumulus phase in olivine-bearing cumulates in MCUs III and IV. The index minerals defining the phase layering are used to divide each MCU into a maximum of 6 cumulate zones (a–f) as outlined in Fig. 8.

Within each megacyclic unit phase layering is accompanied by cryptic layering of mineral compositions with stratigraphic height (Duchesne, 1972; Nielsen and Wilson, 1991; Wilson et al., 1996). The most primitive silicate compositions are found in the leucotroctolitic zones at the base of the MCUs. In the Layered Series the most evolved compositions are found in MCU IVf containing antiperthitic plagioclase and inverted pigeonite. The Fe–Ti oxides also display rhythmic cryptic layering with magnetite exhibiting an increasing $TiO_2$-content and decreasing magnesium, vanadium, nickel and chromium contents with differentiation (Duchesne, 1972; Jensen et al., 1993). The highest-temperature ilmenites are characterized by high hematite contents of up to 19 vol.%, high MgO contents exceeding 4 wt.% as well as elevated chromium and nickel contents (Duchesne, 1972; Duchesne et al., 1999). Due to the strong partitioning of chromium and nickel into the oxides their concentration rapidly fall in both magma and cumulus oxides. MgO in ilmenite gradually decreases to a few tenths of percent in the most evolved cumulates.

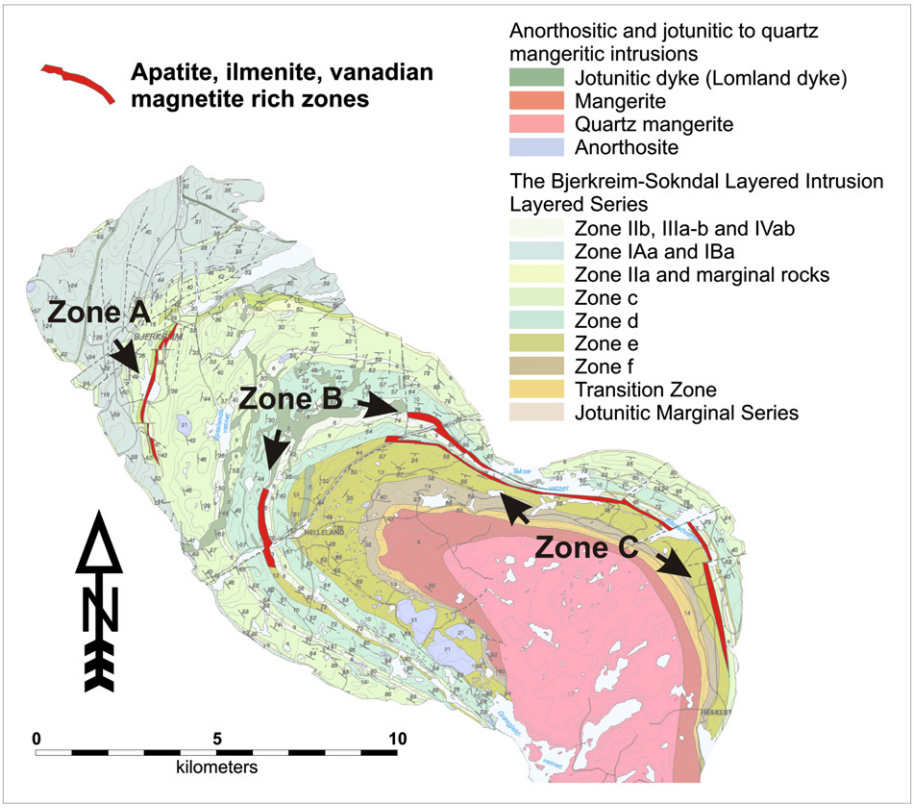


**Fig. 9.** Simplified geological map of the northern (Bjerkreim) lobe of the Bjerkreim–Sokndal Layered Intrusion showing in red the position of the different cumulate zones enriched in apatite, ilmenite and vanadium-rich magnetite. These include Zone A: IBe, Zone B: IIIe and Zone C: IVe.

The BKSK represents a very large, but low-grade resource of apatite, ilmenite and magnetite, carrying significant amounts of vanadium. Detailed maps and knowledge of phase layering and mineral chemistry combined with a predictable stratigraphic control on the resources have made it possible to identify three well constrained zones rich in apatite and oxides. All these zones are located in the northern part of the intrusion, i.e. in the Bjerkreim-lobe (Fig. 9).

In the BKSK apatite is stratigraphically constrained to the e- and f-zones (Fig. 8) which are found in the uppermost part of three of the megacyclic units; MCU IB, MCU III and MCU IV. In these zones, apatite coexists with plagioclase, Ca-poor and Ca-rich pyroxenes, ilmenite and magnetite. The $P_2O_5$ content of the Bjerkreim–Sokndal cumulates correlates with MgO, $TiO_2$ and $Fe_2O_3$, implying that apatite is more abundant in oxide-rich mafic layers (Fig. 5c). The sequences richest in apatite and oxides have been constrained to the lower parts of the apatite-bearing zones and three sequences are evaluated as potential resources. In these potentially ore-grade zones, the coexisting magnetite typically contains around 0.9 wt.% $V_2O_3$ with no apparent stratigraphic variability. Whereas Cr remains low in ilmenite, the MgO-content varies strongly with stratigraphy and the modal composition of the individual layers. Generally the MgO-content decreases as the phase assemblage becomes more evolved, and the MgO-content fluctuates around an average of 1–2 wt.% in the three mineralised zones. EPMA analyses of Fe–Ti oxides in drill cores across the mineralised zone in MCU IV reveal an average of 1.74 wt.% MgO in ilmenite and 0.89 wt.% $V_2O_3$ in magnetite. Apatites are generally fluor-apatites with Cl content below 0.1 wt.%. Apatites from each of the zones have been analysed for REE-content by LA-ICP-MS showing a maximum TREE-content of 0.23 wt.% and averages for the individual sections are in the range of 1400–1484 ppm TREE. The apatites are low in thorium with averages in the range of 1–7 ppm Th (Table 4).

The largest apatite and oxide rich zone is found in MCU IV (Fig. 9). It is estimated to be laterally persistent for more than 10 km and is made up of a stratigraphic sequence 50 m to 170 m thick, but is partly covered by lakes. 38 samples from a number of different traverses across the zone give an average composition of 4.1 wt.% $P_2O_5$ (Max: 5.5%, Min: 2.4%) and 6.2 wt.% $TiO_2$ (Max: 8.5%, Min: 3.8%). A normative recalculation yields an average composition of 10.2% apatite, 12.4% ilmenite and 7.3% magnetite giving a total of 32% of the three value minerals. The data have been confirmed by two drill holes through the MCU-IV mineralised zone at Mjåsund and Ollestad where continuous analyses of 30 m drill cores yield an average of 31% and 27% value minerals, respectively. At the same time, modal analyses of large samples for beneficiation testing, collected at various sites in the mineralised zones, corroborate the calculated normative compositions given here.

The apatite-rich zones of MCU IIIe consist of two isolated parts. The southern part has an estimated thickness of 130 m with a lateral extension of approximately 1500 m. The average normative composition from 9 samples in a profile of 120 m gives 13.4% ilmenite (Min 8.9; Max 15.7), 8.3% apatite (Min 4.7; Max 10.3) and 8% magnetite (Min 5.6; Max 11.5). The northern part of the zone (MCU IIIe) is represented by two profiles 2 km apart. The maximum thickness is 120 m, thinning towards the east to 90 m. The average normative composition from 18 samples in this part of the prospect is 11.4% ilmenite (Min 4.3; Max 17.5), 7.8% apatite (Min 3.8; Max 12.7) and 6.9% magnetite (Min 2.1; Max 11).

The apatite bearing part of MCU IBe forms a 3 km long zone with a maximum thickness of 60 m gradually thinning out at the flanks. The potential extent of the mineralised sequence is poorly documented due to extensive quaternary cover and a challenging topography. The sequence is, however, interesting in terms of the magmatic evolution because the entry of cumulus magnetite is delayed with respect to MCUs III and IV, and magnetite appears at the same time as apatite. Presumably as a result of this the $Fe_2O_3$ contents of the apatite-bearing cumulates are higher than for the equivalent sequences in MCUs III and IV. Based on XRF whole rock analyses from 10 samples in two profiles of

40–50 m each, the average normative abundances of the three minerals have been calculated to 8.3% apatite, 15.2% ilmenite and 10.6% magnetite.

In the Bjerkreim–Sokndal Layered Intrusion the apatite-rich zone of MCU IV is particularly interesting with a considerable exposure of cumulates containing more than 10% normative apatite and 20% Fe–Ti oxides. Future development of the Layered Series as an apatite resource may, however, depend on parallel sales in the widely different market regimes of phosphate, titanium and Fe–V.

### 4.3. Deposits in monzonitic complexes

Enrichment of apatite in association with Fe–Ti oxides typical for the RAP is also a characteristic for members of voluminous plutonic complexes of monzonitic composition developed in both the lower and upper crusts. Thus, they can be subdivided into complexes characterized either by abundant mangerite intrusions or by monzonites. Monzonitic complexes crystallised under granulite facies conditions are found in the Palaeoproterozoic LVMC of northern Norway (Malm and Ormaasen, 1978) and in the late Palaeoproterozoic to early Neoproterozoic mangeritic and jotunitic rocks of the JVNC and MBA of the Caledonides in southern Norway (Fig. 1; Roffeis and Corfu, 2013, and references therein). The apatite occurrences in the two latter areas are poorly known, but appear similar to those in the LVMC and include patchy ultramafic ores and pyroxenitic ores (types given below) with 2–11 wt.% $P_2O_5$ (Neumann, 1985; NGU Ore Database). The LVMC was emplaced during two distinct events at 1870–1860 Ma and 1800–1790 Ma (Corfu, 2004). Most of the apatite deposits are temporally related to quartz normative mangerites of the second and most important magmatic event which represents according to Markl et al. (1998) and Corfu (2004) extraction of magma from the subcontinental mantle and consolidation at a depth of about 15 km (0.4 GPa). According to major element analyses given by Malm and Ormaasen (1978) the mangerites contain an average of about 0.4 wt.% $P_2O_5$. The mangerites of the second event are intruded by alkali basaltic dolerites containing 1.4–2.4 wt.% $P_2O_5$ (Misra and Griffin, 1972). Their relationship to the mangerite magmatism is, however, unclear.

The Oslo Igneous Province (OIP) comprises a number of intrusions with enhanced phosphorus contents, including olivine tholeiitic gabbros, monzodiorites, alkaline troctolites, monzonites and nepheline-rich syenomonzonites. These yield ages in the range 297–256 Ma (Dahlgren et al., 1998; Sundvoll et al., 1990). The plutons crystallised at a depth of 3–4 km below the surface of the former lava plateau, i.e. ~0.1 GPa lithostatic pressure. The monzonitic plutons of the OIP are more enriched in phosphorus in comparison with the mangerites of the LVMC by yielding an average of 0.63 ± 0.25 wt.% $P_2O_5$ (Neumann, 1978). There is also a general enrichment of phosphorus in rocks associated with the monzonites which contain small rafts and larger bodies of monzodiorite and

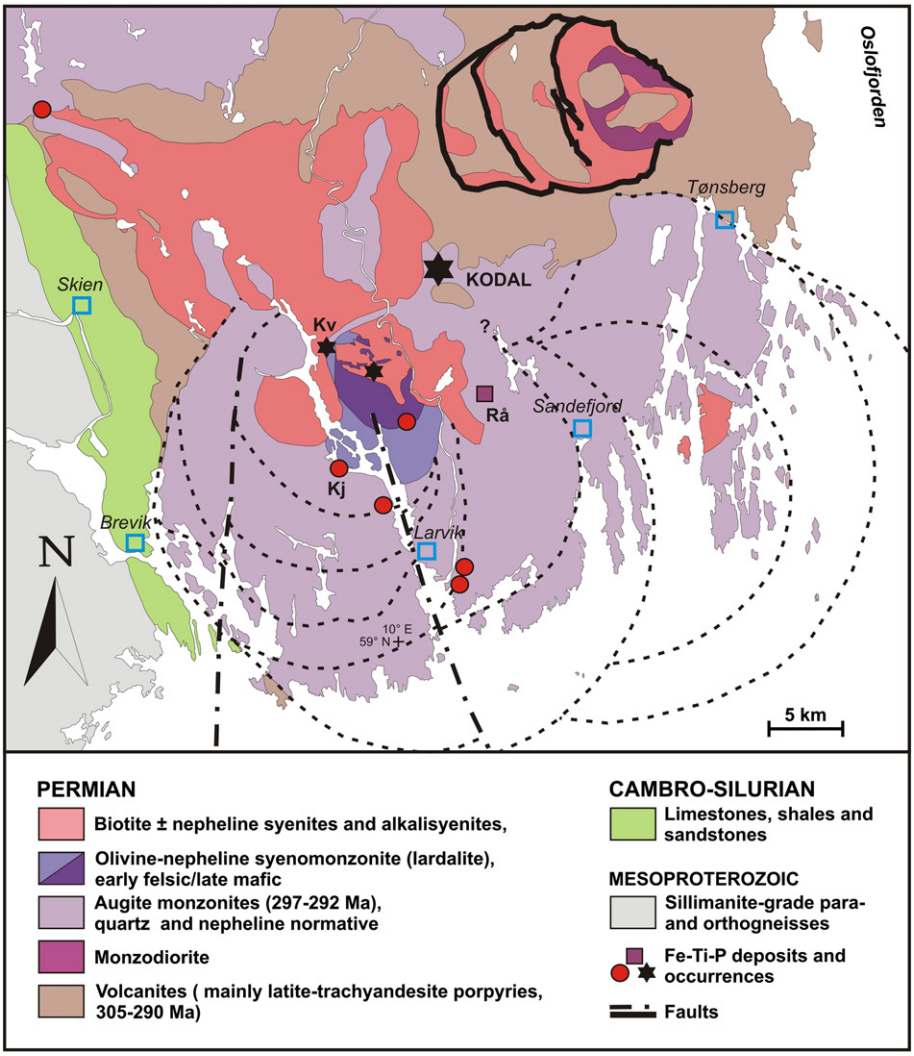


**Fig. 10.** Simplified geological map of the Larvik Plutonic Complex showing the location of different types of apatite ore and the Kodal deposit. Compilation based on Brøgger (1934), Dons and Jorde (1978), Petersen (1978), Lindberg (1985), Berthelsen et al. (1996) and Dahlgren (2004). Black stars = tabular pyroxenitic ores, red symbol = patchy ultramafic ores, and purple square = apatite-rich monzodiorite. Abbreviations: Kj = Kjose, Kv = Kvelde and Rå = Rånerød.

alkaline troctolite (e.g. at Rånerød, Fig. 10), possibly representing cumulates with 1.6–4.7 wt.% $P_2O_5$ (Brøgger, 1934; Barth, 1945; Ihlen, unpublished data). Late stage monzonite dykes in the Larvik Plutonic Complex (Fig. 10) commonly contain more than 1 wt.% $P_2O_5$ (Ihlen, unpublished data). This is the normal level for the nepheline-rich olivine monzonites and syenomonzonites (lardalites) intruding the monzonite massifs in the west where they locally may reach 2 wt.% $P_2O_5$ (Bergstøl, 1972; Oftedahl and Petersen, 1978).

*4.3.1. Apatite–Fe–Ti ores in the Lofoten–Vesterålen Mangerite Complex*

The description of the apatite accumulations in the LVMC is based on the results from an on-going NGU project. They are characterized by large quantities of Fe–Ti oxides comprised by ilmenomagnetite, titanomagnetite and subordinate amounts of ilmenite and hemoilmenite that together far exceeds the amount of apatite. The apatite–Fe–Ti ores are often diluted by silicate gangue comprised by feldspars, clinopyroxene, orthopyroxene, biotite and/or minor zircon and titanite. Three major types of ores can be distinguished which are termed 1) nelsonite, 2) patchy ultramafic, and 3) pyroxenitic. The latter two are also found in the JVNC and OIP.

*Nelsonite* according to the definition by Philpotts (1967) occurs in the LVMC as decimetre to several metre wide veins and breccia dykes intersecting the mangerites and their granulite facies supracrustal wall rocks. The cement of the intrusion breccia at Nordre Følstad (no. 5, Figs. 1 and 5d) are composed of about 85 vol.% Fe–Ti-oxides carrying inclusions and interstitial crystals of fine-grained apatite together with minor biotite and zircon. Monomineralic aggregates of biotite replace the wall-rock feldspars and form a thin veneer separating the Fe–Ti-oxides from the granitic rocks in breccia fragments and feldspar xenocrysts. The field relationships strongly indicate the intrusion of a separate hydrous Fe–Ti–P–Mg melt interacting with the feldspatic granulite wall rocks. Two of the nelsonite deposits in the LVMC yield analytical values in the range of 2.75–4.23 wt.% $P_2O_5$. The nelsonite ores are also enriched in Y and TREE with whole-rock values in the range of 120–229 ppm Y and 984–2329 ppm TREE. Apatite concentrates extracted from the Nordre Følstad ores contain 4616 ppm TREE and 1394 ppm Y (Table 3). The strong enrichment of Zr is a characteristic signature for this type of deposit reaching a maximum of 4345 ppm Zr. Bodies of very biotite-rich (50 vol.%) nelsonitic ores are locally encountered containing up to 0.9 wt.% Zr, but only 1–2 wt.% $P_2O_5$.

*Patchy ultramafic ore* is the most widespread ore type in the mangerites. The mafic minerals filling the interstices between the cm-sized feldspar crystals in the mangerites frequently segregate into irregular ultramafic patches composed mainly of pyroxenes, Fe–Ti oxides, biotite and apatite. The metre-sized segregations of small irregular patches, stringers and schlieren of semi-massive Fe–Ti–P ore grade into the host-rock mangerites via thin zones with intergranular networks (Fig. 5e). These ultramafic segregations have an uneven patchy distribution in up to 100 m wide and more than kilometre long linear zones, frequently close to the border of the individual mangerite plutons. Although the individual semi-massive patches may reach 4.5 wt.% $P_2O_5$, most of the bulk ores are of low grade and rarely exceeds 3 wt.% $P_2O_5$ due to the common dilution by porphyritic feldspar aggregates.

*Pyroxenitic ore* is represented by pyroxene-dominated ultramafites (<40% $SiO_2$) forming bodies composed mainly of fine-grained apatite and Fe–Ti oxides intergrown with pyroxene, biotite and olivine, as well as variable amounts of porphyritic plagioclase and/or alkali feldspar aggregates. These ore bodies may represent cumulate rocks, although their irregular contacts with multiple branches extending into the mangerite host may suggest that they formed as separate intrusions. The ores at Grindvika and adjacent areas (no. 4, Fig. 1) define an *en echelon* array of ore zones, each of them consisting of up to 20 m wide and several hundred metres long zones composed either of a single dyke-like body or of densely spaced lenses, each several metres wide and tens of metres long. Reconnaissance grab-sampling of these ore zones yield analytical values in the range of 2.0–5.5 wt.% $P_2O_5$. Apatite concentrates from the Grindvika ore zone contain 6364 ppm TREE and 630 ppm Y (Table 3). The largest of the mangerite-hosted pyroxenite deposits occurs at Utåker (no. 6) where a 350 m by 700 m and cresent-shaped magnetite-olivine pyroxenite is exposed along the beach. However, only two grab-samples have been analysed so far yielding 3.3–3.4 wt.% $P_2O_5$ (Malm and Ormaasen, 1978; A. Korneliussen, pers. com., 2013).

The existence of potential resources of apatite in the mangerites of the LVMC, JVNC and MBA has just recently been recognized and our knowledge is presently rather immature. Thus it is difficult to make an assessment of their potential based on a restricted number of analysed samples.

*4.3.2. Apatite–Fe–Ti ores in the Larvik Plutonic Complex*

The monzonites of the Larvik Plutonic Complex consist of coarse-grained augite ± biotite ± olivine monzonites frequently containing larvikite zones where cryptoperthitic alkali feldspar with schiller effect occurs. The common alignment of the usually rhomb-shaped feldspars frequently generates a linear fabric in the monzonites that parallels the outer border of the individual plutons. The Larvik Plutonic Complex comprises a series of crescent-shaped monzonite intrusions formed in response to plutonic centres moving successively from the east towards the west (Fig. 10). Concurrently, the monzonite magmas changed composition from quartz normative in the east to nepheline normative in the western half of the complex.

All of the known occurrences of apatite–Fe–Ti ores in the monzonites of the Larvik Plutonic Complex occur inside nepheline-normative monzonites and syenomonzonites in contrast to quartz normative mangerites in the LVMC. The monzonite and olivine–nepheline monzonite (lardalite) intrusions both contain patchy ultramafic ores similar to those in the LVMC. These are invariably found close to the contact of the individual monzonite plutons. Phosphate grades of the patchy ores are similar to those in the LVMC, i.e. generally of low-grade, but with samples of the interior of the semi-massive patches yielding 4.50 wt.% $P_2O_5$ as in the Kjose zone (Fig. 10; Brøgger, 1934). Tabular semi-massive bodies of apatite-rich magnetite clinopyroxenites previously termed jacupirangite by Brøgger (1934) and Bergstøl (1972) are encountered in several places e.g. at Kvelde where ores contain 4.85 wt.% $P_2O_5$ (Fig. 10). However, the most prominent of these are the magnetite pyroxenite bodies constituting the Kodal apatite–Fe–Ti oxide deposit (Fig. 11).

*4.3.2.1. The Kodal deposit.* The Kodal deposit was investigated by Norsk Hydro due to its potential as an apatite raw material for the company's fertilizer plants. Between the years 1959 and 1984 the company conducted three exploration campaigns including 58 drill holes (18 mm), beneficiation tests and apatite resource estimations. Renewed interest for the deposit has recently been taken by Kodal Minerals Ltd. which presently is conducting systematic core drilling according to JORC/PERC standards and advanced ore dressing tests.

The deposit is comprised of a1900 m long ore zone of closely spaced lenses of massive pyroxenitic ores, 18–20 m thick, that have been drilled to a vertical depth of 150 m. The individual ore lenses show sharp contacts with the monzonites in the foot wall and gradational contacts with the monzonites in the hanging wall (Lindberg, 1985). The greyish monzonites, commonly altered to pink varieties along fracture zones, are composed of cm-sized perthitic alkali feldspar and oligoclase, some antiperthitic, which carry interstitial aggregates of augite, hornblende, apatite, Fe–Ti oxides rimmed by biotite, and occasional grains of orthopyroxene (Starmer, 1974). The apatite represents an early liquidus mineral occurring both as scattered inclusions in the feldspar crystals and as densely spaced prisms enclosed by the minerals of the mafic aggregates where it often exceeds 10 vol.%.

The ore zone terminates against a younger intrusion of alkali feldspar syenite in the west, whereas it tapers off in a series of small

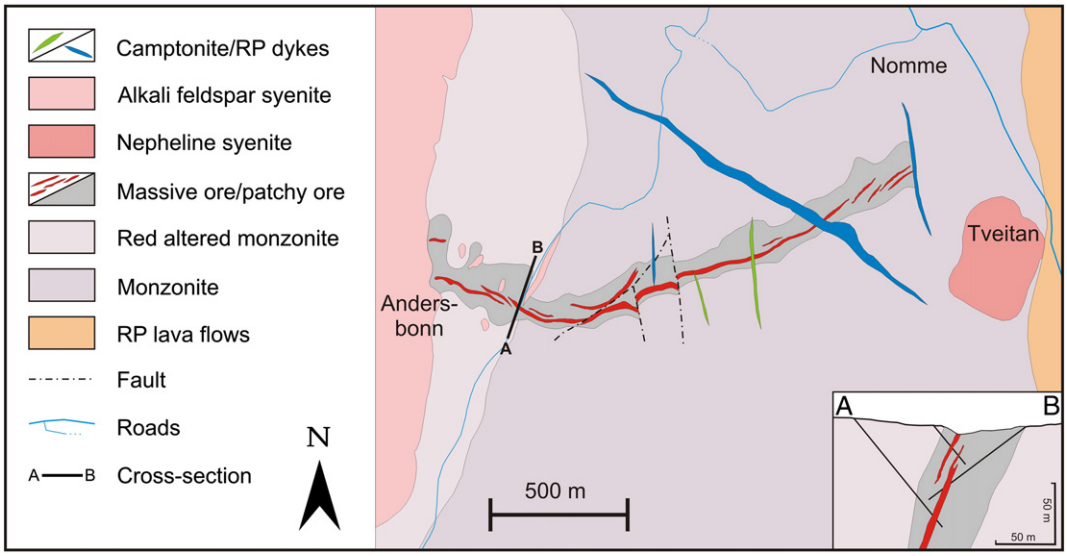


**Fig. 11.** Simplified geological map of the Kodal ore zone with drill-hole section redrawn from Lindberg (1985). RP in the legend: Rhomb porphyry = porphyritic latite-trachyandesite.

*en echelon* lenses in the east. It is enveloped by a transitional zone up to 200 m wide of patchy ores (Fig. 11) composed of widely distributed lenses and more irregularly shaped pods of massive ore that have dimensions from cm to several decametre. The lenses increase in abundance when approaching the main ore zone (Lindberg, 1985). The ore zone shows small fault displacements and is cross-cut by dykes of alkali-feldspar syenite, trachyandesitic porphyry (RP) and camptonite (Fig. 11).

The massive pyroxenitic ores which contain small patches of monzonites are fine-grained with anhedral to subhedral clinopyroxene grains in a matrix of ilmenite, magnetite and apatite, the latter forming 0.1–0.5 mm long prisms and needles occurring interstitially to the Fe–Ti oxides (Bergstøl, 1972). Modal analyses of the ores show the following variations: 15–24% apatite (average 17%), 25–60% ilmenomagnetite and titanomagnetite, 5–15% high-Mg ilmenite, 20–40% diopside, and 3–10% phlogopite, magnesiohastingsitic hornblende, olivine, feldspar, nepheline and carbonates (Andersen and Seiersten, 1994; Bergstøl, 1972; Lindberg, 1985). Biotite is especially enriched along the contact of the ore bodies (Bergstøl, 1972). Fluid inclusions in the apatite are filled with moderately saline $H_2O$–$CO_2$ fluids together with submicroscopic crystals of calcic amphibole, titanite, calcite and REE carbonate (Andersen and Seiersten, 1994). The two latter authors showed on the basis of fluid densities that the apatite crystallised at a pressure in excess of 0.5 GPa, possible as high as 0.8 GPa, i.e. much higher than the lithostatic pressure of 0.1 GPa prevailing during the crystallisation of the host monzonite.

Bergstøl (1972) concluded that the deposit was formed by intrusion of an immiscible Fe–Ti–P melt containing cumulus crystals of clinopyroxene that was emplaced into a not yet fully consolidated monzonite, whereas Lindberg (1985) suggested formation by in situ fractional crystallisation of a monzonitic parent magma. The latest model was given by Andersen and Seiersten (1994) who envisage that the accumulation of apatite and ultramafic cumulates originally occurred in an ijolitic magma in the middle or lower crust. Later these cumulates were captured by ascending monzonite magma and brought to their present position where they re-settled to form semi-continuous layers of cumulate minerals. The present authors prefer the latter model although we have some problems on fully understanding how a large mass of high density cumulate minerals can be transported by a low-density magma from the lower or middle crust to near surface environments.

The Kodal deposit has according to the numbers given by Lindberg (1985) inferred open pit resources of about 70 Mt with an average content of 4.9 wt.% $P_2O_5$ (massive ore + transition zone) or alternatively underground resources of 35 Mt with an average of 6.8 wt.% $P_2O_5$ (massive ore). The apatite in the massive ores of the Kodal deposit shows Th levels acceptable for NKP fertilizer production (Tables 3 and 4), whereas the high TREY contents of about 1 wt.% may represent a potential extra value, if extracted.

## 5. Vein deposits

This type of apatite deposit is only found inside the Sveconorwegian Mobile Belt (SMB). Geological evidence indicates that they developed episodically during the evolution of the Sveconorwegian orogeny (1140–900 Ma) in response to structurally controlled fluid flow.

### *5.1. Kiruna-type apatite–Fe oxide deposits*

Magnetite–hematite deposits occur in several places in the Nissedal area in Telemark (no. 14, Fig. 1) where they comprise massive oxide veins, some of them high in apatite. The host rocks consist largely of amphibolite facies biotite and/or hornblende gneisses representing felsic to intermediate meta-volcanites of assumed early Mesoproterozoic age. The largest of the apatite-bearing deposits at Søftestad was mined for 30 years in the last century (Bugge, 1978). The underground workings followed a linear ore zone composed of three *en echelon* lenses, 2–5 m thick, with a total strike length of about 500 m. The frequently mylonitic ores are oriented at an angle to the regional structural trend of the country rocks. The ore zone comprises alternating massive bands of magnetite and hematite (ratio 3:2), up to 4 m thick, separated by cm to metre thick gneiss bands with disseminated Fe-oxides (Vogt, 1895). Disseminated and mm-thick parallel stringers of fluorapatite are mainly found in the magnetite-dominated ores which contain up to 8 wt.% $P_2O_5$ (Bugge, 1978; Vogt, 1895). The ore mined in the past contained 47–50 wt.% Fe and 1.9–2.4 wt.% $P_2O_5$ (Aamo, 1957). Ore reserves left in the mine were estimated by Bugge (1978) to be in the order of 0.5 Mt with 55 wt.% Fe and 3.9 wt.% $P_2O_5$. Both Vogt (1895) and Bugge (1978) noticed the similarities with the much larger Kiruna-type Fe–P deposits (Gällivarre) in northern Sweden.

### *5.2. Metasomatic deposits*

More than hundred small apatite and/or rutile veins are distributed in the Bamble–Lillesand Block (Fig. 1) where they mainly intersect meta-gabbroic rocks affected by regional scale metasomatism including

scapolitisation, albitisation and/or calc-silicate alteration (Brøgger, 1935; Engvik et al., 2011, and references therein). The apatite veins and lenses are decimetre to several metres thick and rarely exceed 100 min length. They are composed of variable proportions of biotite, amphibole, clinopyroxene, scapolite, apatite, albite, quartz, rutile, calcite, magnetite, pyrrhotite and titanite (Brøgger and Reusch, 1875; Bugge, 1922). The apatite commonly occurs as coarsely crystalline aggregates and local crystals of up to 1 m in length (Brøgger and Reusch, 1875). Comparable veins are widespread in the Nissedal area where they also intersect the sheared ores of the Søftestad deposit and in the areas surrounding the Rossavika deposit in southwestern Norway (no. 16, Fig. 1).

These veins in the Bamble–Lillesand Block are the only ones that have been mined solely for phosphate in Norway. About 50 vein systems were worked from about 1850 to shortly after the first world war when a total of about 250,000 tonnes of apatite were produced, including 160,000 tonnes from the Ødegården deposit (Bugge, 1978). The Ødegården deposit (no. 13, Fig. 1) occurs in a deformed troctolitic leucogabbro dated to 1149 ± 7 Ma that has been scapolitised over a distance of about 1.5 km (Engvik et al., 2011). Metasomatism is centred on and occurs outwards from a system of parallel and up to metre thick apatite–enstantite–phlogopite veins containing about 30 wt.% apatite (Bugge, 1978). Detailed studies by Engvik et al. (2009, 2011) reveal a gradual decrease in apatite content in successive metasomatic zones away from the veins. The composition of apatite changed from fluor-chlorapatite with 1.9 wt.% Cl in the leucogabbro protolith to chlorapatite with up to 6.8 wt.% Cl in the scapolite metagabbros and apatite–phlogopite veins (Engvik et al., 2009). The chlorapatite shows pseudomorphic replacement by hydroxy-fluorapatite containing μm-sized inclusions of monazite, xenotime and allanite (Engvik et al., 2009; Lieftink et al., 1994). LA-ICP-MS analyses of the different types of apatite show that they all are enriched in Y (1481–1919 ppm) whereas the primary fluor-chlorapatite is somewhat higher in TREE (average 5820 ppm) than the others yielding averages of 5106 ppm TREE in the chlorapatite and 5232 ppm TREE in the hydroxy-fluorapatite. The metasomatic overprint on the gabbro intrusion yields a Rb–Sr age of 1068 ± 7 Ma for phlogopite which indicates that the fluid migration at temperatures of ~600–700 °C represents a continuum of the second tectonothermal event (amphibolite facies) in the Bamble–Lillesand Block (Engvik et al., 2011).

The high-grade paragneisses at Rossavika in SW Norway (no. 16, Fig. 1) host an enigmatic apatite-deposit represented by three tabular and dyke-like carbonate lenses which have been explored in the past by trial workings. The lenses which are oriented roughly parallel to the foliation and metamorphic banding of the wall rocks are 3–5 m thick and have a length of more than 50 m along strike and dip (Ihlen, unpublished data). The contact zone is characterized by abundant veinlets and dissemination of alkali feldspar and biotite in both the carbonate rocks and adjacent gneisses; a feature resembling fenitisation. The medium-grained carbonate lenses carry abundant parallel-oriented coarse crystals of apatite in a matrix of calcite and minor chlorite-altered biotite, alkali feldspar, epidote, quartz and titanite. Three grab samples of the lenses yield 7.63–21.34 wt.% $P_2O_5$. Although the calcite lenses look like a deformed carbonatite dyke, they are very low in Th (<1 ppm), Sr (<1384 ppm) and Ba (<278 ppm). An apatite concentrate yields 3806 ppm TREE and 184 ppm Y (Table 3). Thus, the chemical signature of the calcite–apatite lenses does not fit the chemical characteristics of magmatic carbonatites. But stable isotope data ($\delta^{18}O$, $\delta^{13}C$) given by Bol (1990) plot within the fields of magmatic carbonatites (Bell, 2005) and outside the fields for high-grade meta-sedimentary marbles of the area. A possible metasomatic origin is supported by the widespread occurrences of small apatite-rich hornblende veins in the surrounding areas (Ihlen, unpublished data).

## 6. The REE chemistry of apatite

The chondrite normalized patterns for the Fen carbonatites are characterized by flat LREE distribution and comparatively high HREE values resulting in very low $La/Yb_n$ ratios in the range of 28–58 (Andersen, 1987a,b; Hornig-Kjarsgaard, 1998; Mitchell and Brunfelt, 1975; Møller et al., 1980). Apatite concentrates from the Fen carbonatites display a fairly linear steeply dipping REE pattern with strong enrichment in LREE. The resulting $La/Yb_n$ lies between 150 and 160 for both samples presented in Fig. 12a. The trends do show a slight concavity indicative of higher MREE over HREE enrichment compared to LREE over MREE. The two samples have parallel patterns and the apatite cumulate is systematically higher in all REEs than the calcite-carbonatite sample also presented. There are no single anomalies in the patterns and cerium is not obviously affected by coprecipitation of pyrochlor.

The patterns for apatite concentrates from the Lillebukt Complex in the SIP are very similar but even more linear. The fractionation among the REEs is a little less than in the Fen apatite and the pattern somewhat flatter, with $La/Yb_n$ ratios between 90 and 110. Generally the REE content of apatite in the Lillebukt Complex (5601 ppm TREE) is somewhat higher than the maximum value for the Fen Complex (5220 ppm TREE; Hornig-Kjarsgaard, 1998). The apatite concentrate from one of the carbonate lenses in the Rossavika deposit is also linear, but even flatter again with a $La/Yb_n$ ratio of 69. The apatite of Rossavika is similar to those of the Fen Carbonatites in terms of LREE but more enriched in HREE and there is a tendency towards less fractionation among the LREE.

The Misværdal Complex is genetically poorly understood. The REE patterns in collected apatite separates are even flatter than the other alkaline and carbonatitic samples (Fig. 12a). Apatite from fine-grained pyroxenite shows a $La/Yb_n$ ratio of 22 with a flatter pattern than the apatite-rich coarse-grained pyroxenite ($La/Yb_n$ 27–55). However, the most prominent difference in comparison with the alkaline and carbonatitic samples is the lack of, or reversed, fractionation among the LREE. We speculate that this pattern may be related to the secondary growth of strongly LREE-fractionated allanite in the Misværdal Complex. This trend becomes even more apparent when looking at LA-ICP-MS analyses of individual apatite grains (Table 4). Also here there is a generally linear trend with a conspicuous negative La-anomaly and the data now resolve a very poorly defined negative Eu-anomaly (Fig. 13a). The LA-ICP-MS data indicate a more strongly fractionated REE-pattern than the concentrate analyses with $La/Yb_n$ of 51–87, even though the data are overlapping.

Four samples from three different e-zones in the Bjerkreim–Sokndal Intrusion have also been analysed by LA-ICP-MS. The REE patterns of the cumulus apatites are virtually identical and thus not dependent on the megacyclic unit sampled (Fig. 13b). The apatite trends have a flat LREE with a slightly negative La-anomaly and a moderate Eu-anomaly, resulting from the prior fractionation of cumulus plagioclase. The convex pattern curves have previously been used to model a parental melt for the Bjerkreim–Sokndal Intrusion with a linear fractionation pattern across the complete REE-spectrum, $La/Yb_n$ of less than 10, no Eu-anomaly and characteristically low in TREE (Duchesne and Demaiffe 1978). The pattern fits well with the documented patterns found in the fine grained marginal rocks of the intrusion (Duchesne and Hertogen, 1988; Robins et al, 1997).

Apatite concentrates of nelsonite samples from the LVMC and the RAP have very flat and poorly fractionated REE patterns with $La/Yb_n$ ratios of 6–11 (Fig. 12b). In particular the LREE pattern remains conspicuously flat. All samples have a profound negative Eu-anomaly reflecting the importance of plagioclase fractionation in the magmatic evolution of the anorthositic and mangeritic complexes. The same pattern is evident for the apatite concentrate from the pyroxenitic ore at Grindvika, LVMC, (Fig. 12c) showing a flat LREE pattern, distinct Eu-anomaly and modest fractionation across the REE range ($La/Yb_n$ 20). The Grindvika pattern is, however, slightly convex. Again the Eu-anomaly reflects prior plagioclase fractionation, and plagioclase is an early cumulus phase of the primary melts in this type of setting.

The concentrates from the apatite-rich pyroxenite of the Kodal deposit display a slightly convex REE-pattern with a distinct Eu-anomaly (Fig. 12c), but there is now a clear fractionation among the LREE. The

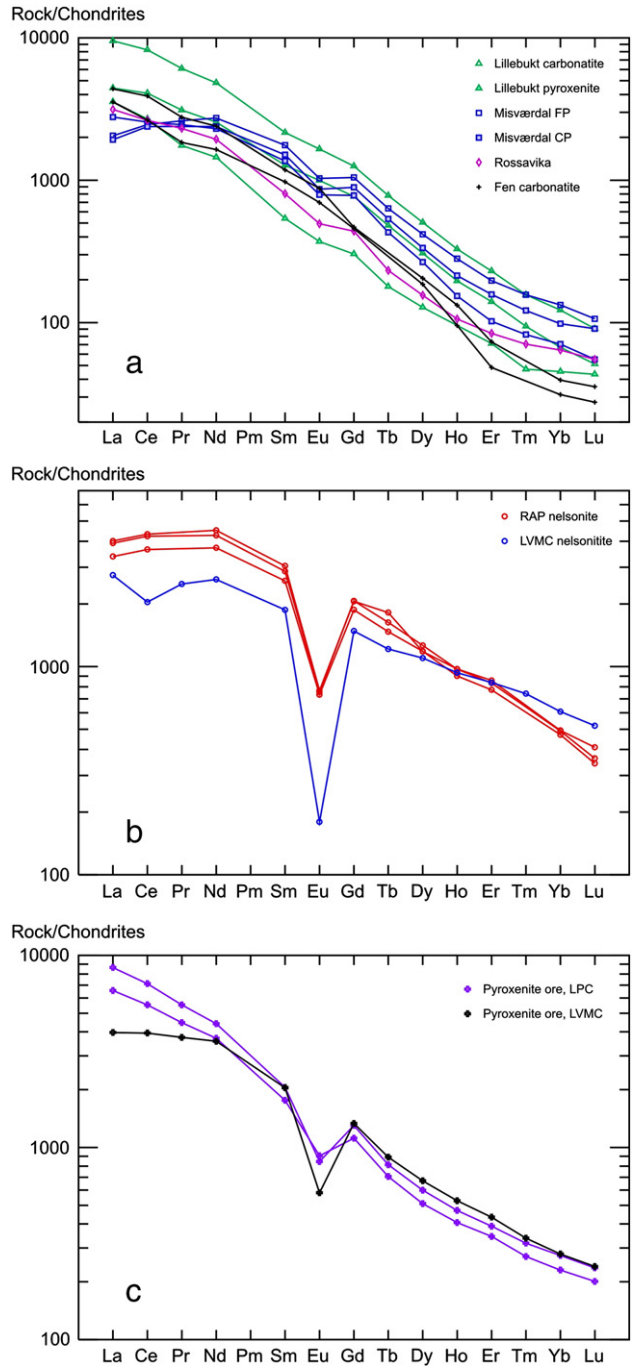


**Fig. 12.** Chondrite-normalized distribution patterns for REE in apatite concentrates (ICP-MS analyses) based on analytical values given in Table 3. a) Apatite in carbonatites and clinopyroxenite dykes of the Lillebukt Complex, in fine- (FP) and coarse-grained pyroxenites (CP) of the Misværdal Complex, in a metasomatic carbonate lens of the Rossavika deposit, and range of values for apatite in calcite-carbonatite of the Fen Complex given by Hornig-Kjarsgaard (1998); b) apatite in nelsonite dykes at Nordre Følstad in LVMC and analytical values given by Duchesne and Schiellerup (2001) for nelsonite dykes in the RAP; c) apatite in magnetite pyroxenitic ores from Grindvika in the LVMC and the Kodal deposit in the Larvik Plutonic Complex (LPC). Chondrite values are taken from Sun and McDonough (1989).

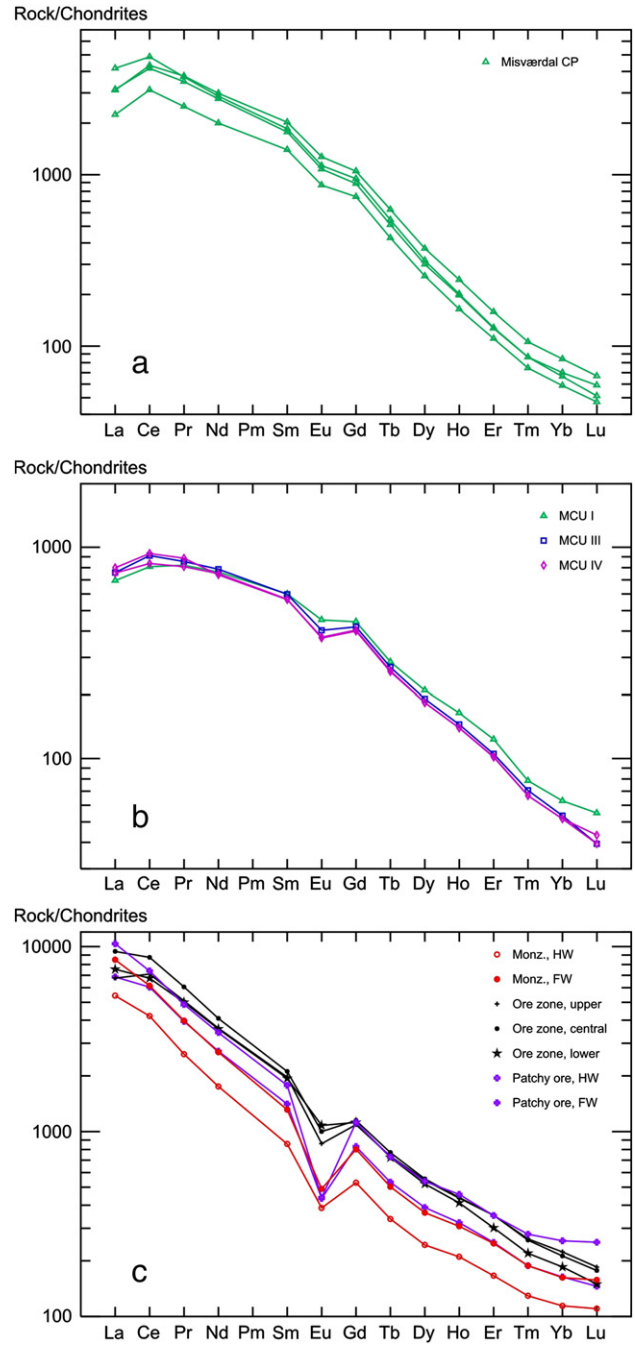


**Fig. 13.** Chondrite-normalized distribution patterns for average REE in apatite grains (5–14) of individual polished sections (LA-ICP-MS analyses) from a) coarse-grained pyroxenites (CP) in the Misværdal Complex, b) MCUs IBe, IIIe and IV of the Bjerkreim–Sokndal Layered Intrusion and from c) the hanging wall (HW) and foot wall (FW) monzonites and patchy ores in the Kodal deposit and from the upper, central and lower parts of the massive ore zone.

total fractionation across the REE spectrum is higher ($La/Yb_n$ 40–44). The Eu-anomaly implies a foregoing plagioclase fractionation, which possibly links the Kodal pyroxenites to the formation of the hosting monzonites, or is inherited from a presumed ijolitic parental melt. However, LA-ICP-MS data for the apatite grains in the various zones of the Kodal deposit reveal a distinctly parallel signature for the ore zones and the foot wall and hanging wall monzonites (Table 4; Fig. 13c). The main difference is the TREE content of the apatites and the size of the negative Eu-anomaly. All patterns for both ore zones and host rock are slightly concave with poor fractionation among the HREE, and all have $La/Yb_n$ between 42 and 73. The apatites from both the massive ore and host monzonites are generally high in REE content and appear to be highest in the ore zone.

## 7. Conclusion

Norway exhibits a wide spectrum of different genetic types of apatite deposits ranging in age from the Palaeoproterozoic to the Permian.

The sedimentary deposits of phosphorites and stratiform volcanogenic Fe–P ores are generally narrow and of low-grade, and their potential resources are very small and comparable to estimated resources of the numerous vein-type deposits (Kiruna-type Fe–P, metasomatic). Major resources of apatite are only found among the igneous deposits comprising alkaline complexes, massif-type anorthosite complexes and monzonitic complexes. The latter two representing apatite–Fe–Ti ores are the most interesting and occur associated with jotunitic intrusions in the RAP, mangeritic intrusions in the LVMC, JVNC and MBA and monzonitic intrusions in the Larvik Plutonic Complex of the OIP. The apatite in the monzonite- and mangerite-associated deposits contains extractable levels of TREE (>6000 ppm), which are higher than the normal levels for TREE in apatite from alkaline complexes (3700–6000 ppm) and much higher than the levels for apatite in the BKSK of the RAP (1400–1500 ppm). The BKSK has resources exceeding 300 Mt with average normative contents of 8.3–10.5% apatite, 12.5–15.2% ilmenite and 21.7–23.5% V-magnetite. The Larvik Plutonic Complex hosting the Kodal deposit contains widespread small occurrences of high-REE apatite ores which are comparable to those in the LVMC, JVNC and MBA where detailed data are missing. The Kodal deposit has ore reserves calculated to 70 Mt with 4.9 wt.% $P_2O_5$ (open pit operation) or alternatively 35 Mt with 6.8 wt.% $P_2O_5$ (underground operation). The Kodal apatite contains about 1 wt.% TREY which may add extra value to the deposit.

## Acknowledgment

The research leading to these results has received funding from the European Community's Seventh Framework Programme ([FP7/2007–2013]) under grant agreement n°309373. This publication reflects only the author's view, exempting the Community from any liability. Project web site: www.bgs.ac.uk/eurare/. Thanks are also due to the staff at the chemical laboratory of the Geological Survey of Norway who has conducted major element XRF-analyses and apatite separation. T. Vrålstad is acknowledged for the helpful discussions during the preparation of the manuscript. We also wish to thank Professor Tom Andersen and an anonymous reviewer for their constructive criticism of the manuscript.

## References

Aamo, A., 1957. Søftestad gruber. Bergverkenes Landssammenslutning gjennom 50 år, 1907–1957. Grøndahl & Søns boktrykkeri, Oslo, pp. 272–274 (in Norwegian).
Aggerholm, V., Parr, S., 1984. Undersøkelse av apatitholdige bergartskompleks ved Tappeluft på Øksfjordhalvøya i Ytre Vest-Finnmark. Nor. Geol. Unders.-Nor. Hydro. Rapp. 25 (13 pp., in Norwegian).
Andersen, T., 1983. Iron ores in the Fen central complex, Telemark (S. Norway): petrography, chemical evolution and conditions of equilibrium. Nor. Geol. Tidsskr. 63, 73–82.
Andersen, T., 1984. Secondary processes in carbonatites: petrology of "rødberg" (hematite–calcite–dolomite carbonatite) in the Fen central complex, Telemark (South Norway). Lithos 17, 227–245.
Andersen, T., 1986a. Compositional variation of some rare earth minerals from the Fen Complex (Telemark, SE Norway): implications for the mobility of rare earths in a carbonatite system. Mineral. Mag. 50, 503–509.
Andersen, T., 1986b. Magmatic fluids in the Fen carbonatite complex, S.E. Norway. Evidence of mid-crustal fractionation from solid and fluid inclusions in apatite. Contrib. Mineral. Petrol. 93, 491–503.
Andersen, T., 1987a. Mantle and crustal components in a carbonatite complex, and the evolution of carbonatite magma. REE and isotope evidence from the Fen complex, S.E. Norway. Chem. Geol. Isot. Geosci. Sect. 65, 147–166.
Andersen, T., 1987b. A model for the evolution of hematite carbonatite, based on whole-rock major and trace element data from the Fen complex, southeast Norway. Appl. Geochem. 2, 163–180.
Andersen, T., 1988. Evolution of peralkaline calcite carbonatite magma in the Fen complex, southeast Norway. Lithos 22, 99–112.
Andersen, T., 1989. Carbonatite-related contact metasomatism in the Fen complex, Norway. Effects and petrogenetic implications. Mineral. Mag. 53, 395–414.
Andersen, T., 2005. Terrane analysis, regional nomenclature and crustal evolution in the Southwest Scandinavian Domain of the Fennoscandian Shield. GFF 127, 159–168.
Andersen, T., Qvale, H., 1986. Pyroclastic mechanisms for carbonatite intrusion. Evidence from intrusives in the Fen central complex, SE Norway. J. Geol. 94, 762–769.
Andersen, T., Seiersten, M., 1994. Deep cumulates in a shallow intrusion: origin and crystallization history of a pyroxenite (jacupirangite s.l.) body in the Larvik Pluton, Oslo Region, South Norway. Neues Jb. Mineral. Monat. 6, 255–274.
Andersen, T., Griffin, W.L., Jackson, S.E., Knudsen, T.-L., 2004. Mid-Proterozoic magmatic arc evolution at the southwest margin of the Baltic Shield. Lithos 73, 289–318.
Andersson, U.B., Sjöström, H., Høgdahl, K., Eklund, O., 2004. The Transscandinavian Igneous Belt, evolutionary models. In: Høgdahl, K., Andersson, U.B., Eklund, O. (Eds.), The Transscandinavian Igneous Belt (TIB) in Sweden: a review of its character and evolution. Geol. Surv. Finland, Spec. Pap., 37, pp. 104–112.
Barnes, C.G., Reid, K., Frost, C.D., Barnes, M.A., Allen, C.M., Yoshinobu, A.S., 2011. Ordovician and Silurian magmatism in the Upper Nappe, Uppermost Allochthon, Helgeland Nappe Complex, north central Norway. Norw. J. Geol. 91, 121–136.
Barth, T., 1927. Die Pegmatitgänge der kaledonischen intrusivegesteine im Seilandgebiete. Skr. Norske Vidensk.-Akad. Oslo, I Mat.-Naturvidensk. Kl. 1927 (8), 1–123.
Barth, T.F.W., 1945. Studies of the igneous rock complex of the Oslo Region, II. Systematic petrography of the plutonic rocks. Skr. Norske Vidensk.-Akad. Oslo, I. Mat.-Naturvidensk. Kl. 1944 (9), 1–104.
Bekker, A., Slack, J.F., Planavsky, N., Krapež, B., Hofman, A., Konhauser, K.O., Rouxel, O.J., 2010. Iron formation. The sedimentary product of a complex interplay among mantle, tectonic, oceanic, and biospheric processes. Econ. Geol. 105, 467–508.
Bell, K., 2005. Carbonatites. In: Selley, R.C., Cocks, L.R.M., Plimer, I.R. (Eds.), Encyclopedia of Geology. Elsevier, Amsterdam, pp. 217–233.
Bennett, M.C., Emblin, S.R., Robins, B., Yeo, W.J.A., 1986. High-temperature ultramafic complexes in the North Norwegian Caledonides: I — regional setting and field relationships. Nor. Geol. Unders. B. 405, 1–40.
Bergstøl, S., 1972. The jacupirangite at Kodal, Vestfold, Norway. Miner. Deposita 7, 233–246.
Bergstøl, S., Svinndal, S., 1960. The carbonatite and per-alkaline rocks of the Fen area — petrology. Nor. Geol. Unders. 208, 99–105.
Berthelsen, A., Olerud, S., Sigmond, E.M.O., 1996. Oslo, bedrock geology map, scale 1:250,000. Nor. Geol. Unders. (in Norwegian).
Bingen, B., Nordgulen, Ø., Viola, G., 2008. A four-phase model for the Sveconorwegian orogeny, SW Scandinavia. Norw. J. Geol. 88, 43–72.
Bjørlykke, H., 1953. Utnytting av Søvemalm. En beriktigelse av L.A. Conradis artikkel. Tidsskr. Kjemi, Bergv., Metall. 4, 47–48 (in Norwegian).
Bjørlykke, K., 1974. Depositional history and geochemical composition of Lower Palaezoic epicontinental sediments from the Oslo region. Nor. Geol. Unders. 305, 1–81.
Bjørlykke, H., Svinndal, S., 1960. The carbonatite and per-alkaline rocks of the Fen area — mining and exploration work. Nor. Geol. Unders. 208, 105–110.
Bjørlykke, K., Elvsborg, A., Høy, T., 1976. Late Precambrian central sparagmite basin of south Norway. Nor. Geol. Tidsskr. 56, 233–290.
Bol, L.C.G.M., 1990. Geochemistry of high-temperature granulitic supracrustals from Rogaland, SW Norway. (Ph.D. thesis) Geol. Ultraiect., 66. Utrecht University, The Netherlands (137 pp.).
Bolle, O., Trindade, R.I.F., Bouchez, J.L., Duchesne, J.C., 2002. Imaging downward granitic magma transport in the Rogaland Igneous Complex, SW Norway. Terra Nova 14, 87–92.
Brøgger, W.C., 1921. Die Eruptivgesteine des Kristianiagebietes IV. Das Fengebiet in Telemark, Norwegen. Skr. Norske Vidensk.-Akad. i Kristiania, Mat.-Naturvitensk. Kl. 1920 (9), 1–408.
Brøgger, W.C., 1934. Die Eruptivgesteine des Oslogebietes. VII. Die chemische Zusammensetzung der Eruptivgesteine des Oslogebietes. Skr. Norske Vidensk.-Akad. i Oslo, I. Mat.-Naturvidensk. Kl. 1933 (1), 1–147.
Brøgger, W.C., 1935. On several Archean rocks from the south coast of Norway. II. The south Norwegian hyperites and their metamorphism. Skr. Norske Vidensk.-Akad. i Oslo, I. Mat.-Naturvidensk Kl. 1934 (1), 1–421.
Brøgger, W.C., Reusch, H.H., 1875. Vorkommen des Apatits in Norwegen. Z. Deut. Geol. Ges. 27, 646–702.
Brown, T.J., Shaw, R.A., Bide, T., Petavratzi, E., Raycraft, E.R., Walters, A.S., 2013. World Mineral Production 2007–2011. Brit. Geol. Surv, Nottingham, UK (76 pp.).
Bugge, C., 1922. Statens apatittdrift i rationeringstiden. Nor. Geol. Unders. 110, 1–34 (in Norwegian).
Bugge, J.A.W., 1948. Rana Gruber. Geologisk beskrivelse av jernmalmfeltene i Dunderlandsdalen. Nor. Geol. Unders. 171, 1–149 (in Norwegian).
Bugge, J.A.W., 1978. Norway. In: Bowie, S.H.U., Kvalheim, A., Haslam, H.W. (Eds.), Mineral Deposits of Europe. Northwest Europe. Inst. Min. Metall.-Mineral. Soc. London, vol. 1. Bartholomew Press, Dorking, pp. 199–249.
Charlier, B., Longhi, J., Vander Auwera, J., Storme, J., Maquil, R., Duchesne, J.C., 2010. Continuous polybaric fractional crystallization of high-alumina basalt parental magmas in the Egersund–Ogna massif-type anorthosite (Rogaland, SW Norway) constrained by plagioclase and high-alumina orthopyroxene megacrysts. J. Petrol. 51, 2515–2546.
Cook, P.J., McIlhinney, M.W., 1979. A reevaluation of the spatial and temporal position of sedimentary deposits in the light of plate tectonics. Econ. Geol. 74, 315–330.
Corfu, F., 2004. U–Pb age, setting and tectonic significance of the anorthosite–mangerite–charnockite–granite suite, Lofoten–Vesterålen, Norway. J. Petrol. 45, 1799–1819.
Dahlgren, S., 1987. The satellitic intrusions in the Fen Carbonatite-Alkaline Rock Province, Telemark, Southeastern Norway. (thesis) Cand. Scient.University of Oslo, Norway (390 pp.).
Dahlgren, S., 2004. Nordagutu, bedrock geology map 1713 IV, scale 1: 50,000. Nor. Geol. Unders.
Dahlgren, S., 2005. Miljøgeologisk undersøkelse av lavradioaktivt slagg fra ferroniobproduksjon ved Norsk bergverk på Søve 1956–1965. Regiongeologen 2005 Rapport 1. (47 pp., in Norwegian).
Dahlgren, S., Corfu, F., Hearman, L., 1998. Datering av plutoner og pegmatitter i Larvik pluton-kompleks, sydlige Oslo Graben, ved hjelp av U-Pb isotoper i zirkon og baddeleyitt. In: Nordrum, F.S. (Ed.), Kongsberg Mineral Symposium 1998. Norsk Bergverkmuseum Skr, 14, pp. 32–39 (in Norwegian with English summary).
Dons, J.A., Jorde, K., 1978. Skien, bedrock geology map, scale 1:250,000. Nor. Geol. Unders. (in Norwegian).
Duchesne, J.C., 1972. Iron–titanium oxide minerals in the Bjerkrem–Sogndal Massif, south-western Norway. J. Petrol. 13, 57–81.

Duchesne, J.C., Demaiffe, D., 1978. Trace elements and anorthosite genesis. Earth Planet. Sci. Lett. 38, 249–272.

Duchesne, J.C., Hertogen, J., 1988. Le magma parental du lopolithe de Bjerkreim–Sokndal (Norvège Méridionale). CR Acad. Sci. Paris 306, 45–48.

Duchesne, J.C., Schiellerup, H., 2001. The iron–titanium deposits. In: Duchesne, J.C. (Ed.), The Rogaland Intrusive Massifs, an Excursion Guide. Norges geologiske undersøkelse Report 2001, 29, pp. 56–75.

Duchesne, J.C., Liégeois, J.-P., Vander Auwera, J., Longhi, J., 1999. The crustal tongue melting model and the origin of massive anorthosites. Terra Nova 11, 100–105.

Elvevold, S., Riginiussen, H., Krogh, E.J., Børklund, F., 1994. Reworking of deep-seated gabbros and associated contact metamorphosed paragneisses in the south-eastern part of the Seiland Igneous Province, northern Norway. J. Metamorph. Geol. 12, 539–556.

Engvik, A.K., Golla-Schindler, U., Berndt, J., Austrheim, H., Putnis, A., 2009. Intragranular replacement of chlorapatite by hydroxy-fluor-apatite during metasomatism. Lithos 112, 236–246.

Engvik, A.K., Mezger, K., Wortelkamp, S., Bast, B., Corfu, F., Korneliussen, A., et al., 2011. Metasomatism of gabbro-mineral replacement and element mobilization during the Sveconorwegian metamorphic event. J. Metamorph. Geol. 29, 399–423.

Farrow, C., 1974. The Geology of the Skjerstad Area, Nordland, North Norway. (Ph.D thesis) University of Bristol, UK (230 pp.).

Foslie, S., 1949. Håfjellsmulden i Ofoten og dens sedimentære jern-mangan-malmer. Nor. Geol. Unders. 174, 1–129 (in Norwegian).

Gautneb, H., 2010. Geochemistry and REE distribution of apatite from pyroxenite and carbonatite from the Lillebukt Complex, Stjernøy, Finmark, Northen Norway. Norges geologiske undersøkelse Report 2010.004. (7 pp.).

Gautneb, H., Ihlen, P.M., 2009. The Lillebukt Complex, and adjacent areas, Stjernøy Northern Norway: REVIEW of geology and distribution of phosphorus. Norges geologiske undersøkelse Report 2009.060. (42 pp.).

Geis, H.P., 1967. Die Stellung der norwegische Eisenerzlagerstatte Andørja in der kaledonische geosynklinale. Geol. Rundsch. 56, 561–567.

Gorbatschev, R., 2004. The Transscandinavian Igneous Belt — introduction and background. In: Høgdahl, K., Andersson, U.B., Eklund, O. (Eds.), The Transscandinavian Igneous Belt (TIB) in Sweden: a review of its character and evolutionGeol. Surv. Finland Spec. Pap. 37, 9–15.

Heier, K.S., 1961. Layered gabbro, hornblendite, carbonatite and nepheline syenite on Stjernøy, North Norway. Nor. Geol. Tidsskr. 41, 109–155.

Hornig-Kjarsgaard, I., 1998. Rare earth elements in sövitic carbonatites and their mineral phases. J. Petrol. 39, 2105–2121.

Ihlen, P.M., 2009. Lithochemical investigations of potential apatite resources in the Misværdal and Hopsfjellet ultramafic massifs, northern Norway. Norges geologiske undersøkelse Report 2008.074. (57 pp.).

Ihlen, P.M., Furuhaug, L., 2012. Borkakspr øvetaking av apatitt-førende bergarter i Misværdal pyroksenittmassiv, Bodø kommune, Nordland. Norges geologiske undersøkelse Rapport 2011.069. (95 pp., in Norwegian).

Ilyin, A.V., 1989. Apatite deposits in the Khibiny and Kovdor alkaline igneous complexes, Kola peninsula, Nortwestern USSR. In: Notholt, A.J.G., Sheldon, R.P., Davidson, D.F. (Eds.), Phosphate deposits of the world. Phosphate Rock Resources, vol. 2. Cambridge University Press, Cambridge, pp. 485–493.

Jasinski, S.M., 2011. Phosphate rock. US Geol. Surv. minerals information, Miner. Yearb. Metals and Minerals, vol. 1 (11 pp.).

Jasinski, S.M., 2013. Phosphate rock statistics and information. US Geol. Surv. Mineral Commodity Summaries. (Jan. 2013, 2 pp.).

Jensen, J.C., Nielsen, F.M., Duchesne, J.C., Demaiffe, D., Wilson, J.R., 1993. Magma influx and mixing in the Bjerkreim–Sokndal layered intrusion, South Norway: evidence from the boundary between two megacyclic units at Storeknuten. Lithos 29, 311–325.

Le Maitre, R.W. (Ed.), 2002. Igneous Rocks. A Classification and Glossary of terms, 2nd ed. Cambridge University Press, Cambridge (236 pp.).

Lie, A., Østergaard, K., 2011a. The Fen carbonatite complex, Ulefoss, South Norway. Results and conclusions from preliminary microscope and microprobe studies. 21st North Report. (http://www.reeminerals.no/no/OM-OSS/Geologirapporter/, 35 pp.).

Lie, A., Østergaard, K., 2011b. The Fen carbonatite complex, Ulefoss, South Norway. Summary of historic work and data. 21st North Report. (http://www.reeminerals.no/no/OM-OSS/Geologirapporter/, 47 pp.).

Lieftink, D.J., Nijland, T.G., Maijer, C., 1994. The behavior of rare-earth elements in high-temperature Cl-bearing aqueous fluids: results from the Ødegårdens Verk natural laboratory. Can. Mineral. 32, 149–158.

Lindahl, I., Priesemann, F.D., 1999. Jernmalmen på Andørja, Ibestad kommune-Vurdering av kvalitet på superslig og apatittkonsentrater. Norges geologiske undersøkelse Rapport 99.115. (20 pp., in Norwegian).

Lindberg, P.A., 1985. Fe–Ti–P mineralizations in the Larvikite–lardalite complex, Oslo Rift. In: Korneliussen, A., Robins, B. (Eds.), Titaniferous magnetite, ilmenite and rutile deposits in Norway. Norges geologiske undersøkelse B, 402, pp. 93–98.

Longhi, J., 2005. A mantle or mafic crustal source for Proterozoic anorthosites? Lithos 83, 183–198.

Longhi, J., Vander Auwera, J., Fram, M., Duchesne, J.C., 1999. Some phase equilibrium constraints on the origin of Proterozoic (Massif) anorthosites and related rocks. J. Petrol. 40, 339–362.

Malm, O.A., Ormaasen, D.E., 1978. Mangerite–charnockite intrusives in the Lofoten–Vesterålen area, North Norway. Petrography, chemistry and petrology. Nor. Geol. Unders. 338, 83–114.

Marker, M., Schiellerup, H., Meyer, G., Robins, B., Bolle, O., 2003. Rogaland Anorthosite Province — syntheses. In: Duchesne, J.-C., Korneliussen, A. (Eds.), Ilmenite Deposits and Their Geological Environment. Norges geologiske undersøkelse, Spec. Publ., 9, pp. 109–116.

Markl, G., Frost, B.R., Bucher, K., 1998. The origin of anorthosite and related rocks from the Lofoten islands, northern Norway: I. Field relations and estimation of intrinsic variables. J. Petrol. 39, 1425–1452.

Meert, J.G., Torsvik, T.H., Eide, E.A., 1998. Tectonic significance of the Fen Province, S. Norway. Constraints from geochronology and paleomagnetism. J. Geol. 106, 553–564.

Melezhik, V.A., Zwaan, B.K., Motuza, G., Roberts, D., Solli, A., Fallick, A.E., et al., 2003. Isotope chemostratigraphy combined with a detailed mapping of high-grade marble sequences. Progress towards a new generation of geological maps in metamorphic terranes. Norw. J. Geol. 83, 209–242.

Misra, S.N., Griffin, W.L., 1972. Geochemistry and metamorphism of dolerite dikes from Austvågøy in Lofoten. Nor. Geol. Tidsskr. 52, 409–425.

Mitchell, R.H., 2005. Carbonatites and carbonatites and carbonatites. Can. Mineral. 43, 2049–2068.

Mitchell, R.H., Brunfelt, A.O., 1975. Rare earth element geochemistry of the Fen alkaline complex, Norway. Contrib. Mineral. Petrol. 52, 247–259.

Møller, P., Morteani, G., Schley, F., 1980. Discussion of REE distribution patterns of carbonatites and alkalic rocks. Lithos 13, 171–179.

Mørk, M.B.E., Stabel, A., 1990. Cambrian Sm–Nd dates for an ultramafic intrusion and for high-grade metamorphism on the Øksfjord peninsula, Finnmark, North Norway. Nor. Geol. Tidsskr. 70, 275–291.

Neumann, E.-R., 1978. Petrology of the plutonic rocks. In: Dons, J.A., Larsen, B.T. (Eds.), The Oslo Paleorift. Part I. A review. Nor. Geol. Unders., 337, pp. 25–34.

Neumann, H., 1985. Norges mineraler. Nor. Geol. Unders. Skr. 68 (278 pp., in Norwegian).

Nielsen, F.M., Wilson, J.R., 1991. Crystallization processes in the Bjerkreim–Sokndal layered intrusion, south Norway: evidence from the boundary between two macrocyclic units. Contrib. Mineral. Petrol. 107, 403–414.

Oftedahl, C., Petersen, J.S., 1978. Southern part of the Oslo Rift. In: Dons, J.A., Larsen, B.T. (Eds.), The Oslo Paleorift, part II. Guide to excursions. Norges geologiske undersøkelse, 337, pp. 163–182.

Paludan, J., Hansen, U.B., Olesen, N.Ø., 1994. Structural evolution of the Precambrian Bjerkreim–Sokndal intrusion, South Norway. Nor. Geol. Tidsskr. 74, 185–198.

Pedersen, R.B., Dunning, G.R., Robins, B., 1989. U–Pb ages of nepheline syenite pegmatites from the Seiland Magmatic Province. In: Gayer, R.A. (Ed.), The Caldonide Geology of Scandinavia. Graham & Trotman Ltd., London, pp. 3–8.

Petersen, J.S., 1978. Structure of the larvikite–lardalite complex, Oslo region, Norway, and its evolution. Geol. Rundsch. 67, 330–342.

Philpotts, A.R., 1967. Origin of certain iron–titanium oxide and apatite rocks. Econ. Geol. 62, 303–315.

Puustinen, K., Kauppinen, H., 1989. The Siilinjärvi carbonatite complex, eastern Finland. In: Notholt, A.J.G., Sheldon, R.P., Davidson, D.F. (Eds.), Phosphate deposits of the world. Phosphate Rock Resources, vol. 2. Cambridge University Press, Cambridge, pp. 394–397.

Ramberg, I.B., 1973. Gravity studies of the Fen complex, Norway, and their petrological significance. Contrib. Mineral. Petrol. 38, 115–134.

Roberts, D., 1973. Hammerfest, bedrock geology map, scale 1:250,000. Nor. Geol. Unders. (in Norwegian).

Roberts, D., 1988. The terrane concept and the Scandinavian Caledonides: a synthesis. Nor. Geol. Unders. B. 413, 93–99.

Roberts, D., Gee, D.G., 1985. An introduction to the structure of the Scandinavian Caledonides. In: Gee, D.G., Sturt, B.A. (Eds.), The Caldonides of Scandinavia and Related Areas. John Wiley & Sons, Chichester, pp. 55–68.

Roberts, R.J., Corfu, F., Thorsvik, T.H., Heteringthon, C.J., Ashwal, L.D., 2010. Age of alkaline rocks in the Seiland Igneous Province, Northern Norway. J. Geol. Soc. London 167, 71–81.

Robins, B., 1982. The geology and petrology of the Rognsund intrusion, West Finnmark, northern Norway. Nor. Geol. Unders. 377, 1–55.

Robins, B., 1985. Disseminated Fe–Ti oxides in the Seiland magmatic province of Northern Norway. In: Korneliussen, A., Robins, B. (Eds.), Titaniferous magnetite, ilmenite and rutile deposits in Norway. Norges geologiske undersøkelse B, 402, pp. 79–91.

Robins, B., 1996. Field trip guidebook part II: the Seiland Igneous Province, North Norway. IGCP Project 336, 1996 Field Conference and Symposium, Layered Mafic Complexes and Related Ore Deposits of Northern Fennoscandia: Finland, Norway, Russia. University of Bergen, Norway (33 pp.).

Robins, B., Gardner, P.M., 1974. Synorogenic layered basic intrusions in the Seiland Petrographic Province, Finnmark. Nor. Geol. Unders. 312, 91–130.

Robins, B., Tysseland, M., 1983. The geology, geochemistry and origin of ultrabasic fenites associated with the Pollen carbonatite (Finmark, Norway). Chem. Geol. 40, 65–95.

Robins, B., Tumyr, O., Tysseland, M., Garmann, L.B., 1997. The Bjerkreim–Sokndal layered intrusion, Rogaland, SW Norway: evidence from marginal rocks for a jotunite parent magma. Lithos 39, 121–133.

Roffeis, C., Corfu, F., 2013. Caledonian nappes of southern Norway and their correlation with Sveconorwegian basement domains. In: Corfu, F., Gasser, D., Chew, D.M. (Eds.), New perspectives on the Caledonides of Scandinavia and Related Areas. Geol. Soc. London, Spec. Publ., 390. http://dx.doi.org/10.1144/Sp390.13 (29 pp.).

Sæther, E., 1957. The alkaline rock province of the Fen area in southern Norway. Kgl. Norske Vitensk. Selsk. Skr. 1957 (1), 1–148.

Schärer, U., Wilmart, E., Duchesne, J.C., 1996. The short duration and anorogenic character of anorthosite magmatism: U–Pb dating of the Rogaland complex, Norway. Earth Planet. Sci. Lett. 139, 335–350.

Schiellerup, H., Korneliussen, A., Heldal, T., Marker, M., Bjerkgård, T., Nilsson, L.-P., 2003. Mineral resources in the Rogaland Anorthosite Province, South Norway: origins, history and recent developments. In: Duchesne, J.C., Korneliussen, A. (Eds.), Ilmenite Deposits and Their Geological Environment. Norges geologiske undersøkelse, Spec. Publ., 9. Elsevier Science B.V., Amsterdam, pp. 117–135.

Schiellerup, H., Lambert, R., Prestvik, T., Robins, B., McBride, J., Larsen, R., 2000. Re–Os isotopic evidence for a lower crustal origin of massif-type anorthosites. Nature 405, 781–784.

Skogen, J.H., 1980a. Lillebukt alkaline kompleks: Karbonatittens indre struktur og dens metamorfe og tektoniske utvikling. (Ph.D. thesis) University of Bergen, Norway (170 pp., in Norwegian).

Skogen, J.H., 1980b. The structural evolution of the Lillebukt carbonatite, Stjernoey, Norway. Lithos 13, 221.
Slagstad, T., Roberts, N.M.W., Marker, M., Røhr, T.S., Schiellerup, H., 2013. A non-collisional, accretionary Sveconorwegian orogen. Terra Nova 25, 30–37.
Solli, A., Farrow, C.M., Gjelle, S., 1992. Misvær, bedrock geology map 2029 II, scale 1:50,000. Nor. Geol. Unders.
Starmer, I., 1974. The terminations of the jacupirangite vein at Kodal, Vestfold. Nor. Geol. Unders.-Nor. Hydro. Rep. 60 (5 pp.).
Strand, T., 1929. The Cambrian beds of the Mjøsa district in Norway. Nor. Geol. Tidsskr. 10, 308–365.
Strand, T., 1981. Lillebukt alkaline kompleks, karbonatittens mineralogi og petrokjemi. (Ph.D. thesis) University of Bergen, Norway (249 pp., in Norwegian).
Sturt, B.A., Ramsay, D.M., 1965. The alkaline complex of the Breivikbotn area, Sørøy, northern Norway. Nor. Geol. Unders. 231, 1–142.
Sun, S.-S., McDonough, W.F., 1989. Chemical and isotopic systematics of oceanic basalts: implications for mantle composition and processes. In: Saunders, A.D., Norry, M.J. (Eds.), Magmatism in the Ocean Basins. Geol. Soc. London, Spec. Publ., 42, pp. 313–345.
Sundvoll, B., Neumann, E.-R., Larsen, B.T., Tuen, E., 1990. Age relations among Oslo Rift magmatic rocks. Implications for tectonic and magmatic modelling. Tectonophysics 178, 67–87.
Svinndal, S., 1970. Undersøkelser etter sjeldne jordartselementer (RE) i Fensfeltet, Ulefoss. Nor. Geol. Unders. Rapp. 966 (18 pp., in Norwegian).
Tørudbakken, B.O., Brattli, B., 1985. Ages of metamorphic and deformational events in the Beiarn Nappe Complex, Nordland, Norway. Nor. Geol. Unders. B. 399, 27–39.
Vander Auwera, J., Bolle, O., Bingen, B., Liégeois, J.-P., Bogaerts, M., Duchesne, J.C., et al., 2011. Sveconorwegian massif-type anorthosites and related granitoids result from post-collisional melting of a continental arc root. Earth Sci. Rev. 107, 375–397.
Verschure, R.H., Maijer, C., 2005. A new Rb–Sr isotopic parameter for metasomatism, Δt, and its application in a study of pluri-fenitized gneisses around the Fen ring complex, South Norway. Nor. Geol. Unders. B. 445, 45–71.
Vogt, J.H.L., 1895. Nissedalen jernmalmforekomst (i Telemarken). Nor. Geol. Unders. 17, 1–58 (in Norwegian with German summary).
Vogt, T., 1967. Fjellkjedestudier i den østlige del av Troms. Nor. Geol. Unders. 248, 1–59 (in Norwegian).
Vrålstad, T., 1976. Fosfat i Dividalsgruppen i Reisadalen, Troms. Nor. Geol. Unders.-Nor. Hydro. Rapp. 93 (10 pp., in Norwegian).
Wilson, J.R., Robins, B., Nielsen, F.M., Duchesne, J.C., Vander Auwera, J., 1996. The Bjerkreim–Sokndal layered intrusion, southwest Norway. In: Cawthorn, R.G. (Ed.), Layered Intrusions. Elsevier Science B.V., Amsterdam, pp. 231–256.